Case Studies in Construction Materials 18 (2023) e01849

Contents lists available at ScienceDirect

Case Studies in Construction Materials

journal homepage: www.elsevier.com/locate/cscm

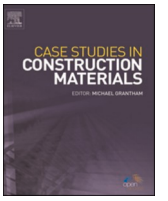

# Post-restoration seismic performance assessment of a historic hypostyle mosque in Anatolia (13th century AD)

Turgay Cosgun [a], Aslı Er Akan [b], Oguz Uzdil [c], Arzu Er [d], Hilal Tuğba Örmecioğlu [e], Baris Sayin [a,*]

[a] Department of Civil Engineering, Istanbul University-Cerrahpasa, Istanbul, Turkey
[b] Department of Architecture, Çankaya University, Ankara, Turkey
[c] Institute of Graduate Sciences, Istanbul University-Cerrahpasa, Istanbul, Turkey
[d] Vocational School of Higher Education, Akdeniz University, Antalya, Turkey
[e] Department of Architecture, Akdeniz University, Antalya, Turkey

ARTICLE INFO

*Keywords:*
Cultural heritage
Masonry Mosque
Asia-Byzantine technique
Nonlinear analysis
Kinematic analysis

ABSTRACT

Assessment of structural performance under seismic effects is a very important step for restoration process of historic buildings that represent construction techniques and material characteristics of their era. This process consists of three stages namely, on-site examinations, restoration practices, and seismic analysis, and therefore, requires a multidisciplinary approach. Hypostyle structures are mostly timber-framed buildings with masonry walls on two or three facades. This construction method is a combination of Asia (wooden pillar) and Byzantine (masonry walls) techniques. The primary load-bearing system in these buildings is composed of multiple rows of wooden pillars. This paper presents post-restoration seismic assessment of a historic wooden hypostyle mosque complex constructed in 1273. This mosque complex is an important structure representing wooden hypostyle architecture in the Anatolia region of Turkey and is composed of three separate structures namely, a main mosque building, a minaret, and a tomb. Linear performance analysis, displacement-controlled nonlinear analysis, and kinematic limit analysis for failure mechanisms were conducted for the structures after the restoration. The linear performance analysis results indicated that the structures meet shear strength requirements for DD3 and DD2 earthquakes with recurrence periods of 72 and 475 years, respectively. Furthermore, according to the linear and non-linear analyses, the complex was found to satisfy performance limits for both ground motion levels in terms of inter-story drifts.

## 1. Introduction

Performance assessment of historic buildings under earthquake loads is composed of three main stages namely, obtaining geometric and mechanical data, modeling the structure using a proper numeric modeling method for these architectural data, and seismic analyses using proper analysis method for the assessment. To determine the mechanical properties of the materials used in these buildings, which is necessary to manage assessment and restoration processes, two different detection approaches, destructive and non-destructive methods can be used. On the other hand, detection of the mechanical properties of the materials used in masonry

* Corresponding author.
*E-mail address:* barsayin@iuc.edu.tr (B. Sayin).

https://doi.org/10.1016/j.cscm.2023.e01849
Received 2 December 2022; Received in revised form 30 December 2022; Accepted 12 January 2023
Available online 14 January 2023

buildings can be very challenging due to a number of reasons including highly variable nature of these materials, lack of experts, and high cost. Such buildings with historical importance were mostly constructed using calcite-based heterogeneous materials with complex geometries. Plus, limestone materials used in such structures are subject to deterioration due to physical, chemical, and biological factors, as well as air pollution [1–4].

Anatolia hosts many historic and cultural heritage structures. Depending on the local materials available at that time, different construction systems and techniques were used in these structures. The majority of these structures were masonry buildings. However, some unique construction systems represent the cultures and characteristics of their time. One of these systems, wooden hypostyle is a frequently used technique during the Seljuk period. Seljuqs are Turkic nomadic tribes that migrated from central Asia to Anatolia. They established an Empire and ruled the Eastern Islamic region between the 11th and 14th centuries [5]. Seljuqs left many great architectural edifices made up of adobe, brick, stone, and wood in Iran and Anatolia. As Oktaç Beycan (2018) conveyed "the structural use of adobe and brick has been widespread in Middle Asia, Turkistan, and Horasan where the resident life of Turks has begun". These materials and construction know-how were transferred to Anatolia with the Seljukian architecture. [6–8]. For instance, the ancient city of Merv, which was also the capital of the great Seljuk Empire, hosts some of the oldest and most important examples of adobe architecture [9]. In addition to Greater Kyz Kala (7th-12th centuries), Lesser Kyz Kala (6th-7th centuries), and Muhammad ibn Zayd Mausoleum (c. 1140) in Merv, the Fortress walls of Ak Kala and Tash-Kala in Kunya-Urgench are also the significant examples of Seljukian adobe architecture. The hypostyle construction method consists of design, wooden columns, and masonry walls. This construction style has its roots in pre-Islamic architectural traditions [10]. This approach was mostly preferred in Anatolian mosques [11–15]. Therefore, the emergence of this construction method in Anatolia dates back to 13th century. In hypostyle mosques, minarets were usually built using wood materials. In general, a mosque design aims to provide wide spans and large spaces. In the hypostyle technique, thin rectangular columns are used in a basilica-like plan to offer large spaces [16]. The most important examples of mosques with hypostyle construction are *Konya Sahip Ata* Mosque (1258), *Sivrihisar Ulu* Mosque (13th century), Beyşehir Esrefoglu Mosque (1297), *Kastamonu Kasaba Koy* Mosque (1367), and *Ankara Arslanhane* Mosque (13th century). Among these structures, *Beyşehir Eşrefoğlu* Mosque inscribed on the tentative list of UNESCO World Heritage sites [17].

Considering the construction date of hypostyle structures, the existence of time-dependent durability and strength losses are inevitable. Besides, the original architecture of some of these buildings was changed and unqualified additions were made [18,19]. In such cases, reconstruction work should be carried out to ensure continuity of the historic and cultural values. Restoration decisions, on the other hand, aim to achieve maximum protection and repair with minimum cost considering economic conditions as well as repairing existing damages with minimum intervention to the original building [20]. When completing the missing parts of a historic building, attention should be paid not only to the harmony in the building as a whole but also to making a distinguishable intervention to the original building. Since the main goal of interventions in such buildings is to protect the aesthetic and historic value of the building, original construction elements and valid documents must be employed. On the other hand, when traditional methods are not sufficient, contemporary techniques confirmed by scientific evidence and tests can be used for protection and retrofitting purposes [21–23]. In this context, Article 10 of the Venice Charter states "Where traditional techniques prove inadequate, the consolidation of a monument can be achieved by the use of any modern technique for conservation and construction, the efficacy of which has been shown by scientific data and proved by experience" [24]. Furthermore, the Charter [25] also says "restoration and reconstruction should reveal culturally significant aspects of the place". Simply, the Charter emphasizes that a restoration decision can be considered necessary when there is enough evidence of an earlier state of the architectural structure.

Before carrying out a restoration practice based on the original architecture of the building, its seismic performance should also be determined based on the currently available information. Underestimating this step can create a structural safety risk, especially for structures that are likely to be exposed to earthquake loads. Therefore, various structural analysis methods; namely, linear, nonlinear, and kinematic analyses can be used for seismic examination of such buildings. The first two analysis methods determine the global behavior of a building, whereas, the last one provides information about local collapse behaviors. In this context, Shariq et al. [26] used the linear time-history analysis method to evaluate the seismic performance of a building. Similarly, Sayin et al. [27] performed linear analysis for a three-story masonry building and presented strengthening proposals based on the analysis results. De Silva et al. [28] introduced a method including specific information about masonry buildings and therefore aimed to determine the seismic performance of the masonry structures. Gunes et al. [29] conducted a comprehensive analysis to assess the current state of a historical building constructed above a historical ruin. Akan et al. [30] examined a restoration work for a hypostyle mosque and determined the structural performance of the restored structure by linear, nonlinear, and kinematic analyses. Similarly, Yildizlar [31] also presented a seismic evaluation of a masonry education building through various numerical approaches. Betti and Galano [32] prepared a 3D finite element model of a historic masonry Palace and determined its seismic performance using static and pushover analyses according to the Italian Technical Specification. Milani and Venturini [33] examined a masonry church and determined the behavior at failure and the overall strength through Monte Carlo simulations. Furthermore, Akcay et al. [34] conducted a comprehensive study including laboratory and numerical examinations and determined the seismic resistance of a three-story masonry building. Their results indicated that the shear stress of the building exceeded the limit values outlined in the code. They, therefore, proposed strengthening practices for walls and slabs to improve the out-of-plane strength of the building. Moreover, Özen [35] performed linear and nonlinear analyses for a masonry building and found that both analyses indicated possible damage to the same section of the building. However, the author argued that the linear analysis would be sufficient since nonlinear analysis takes more time. Betti and Vignoli [36] examined historic masonry buildings through static and dynamic linear and nonlinear analyses and assessed the seismic performance of a basilica-type church which was subjected to seismic loading. Milani et al. [37] conducted kinematic limit analysis for masonry buildings under seismic loads. Palazzi et al. [38] used kinematic limit analyses to determine the main collapse mechanisms and seismic behavior of a church building. Their results indicated that the seismic resistance is insufficient due to the slenderness of the building


**Fig. 1.** The views of the mosque before the restoration. (a) Entrance, (b) Perspective.


**Fig. 2.** Plan and elevations of *Atabey Gazi* Mosque [66].

components.

Asteris et al. proposed a methodology for seismic resistant designs considering the difficulties in numerical modeling to accurately represent masonry buildings. They tested their model on masonry buildings in three different countries namely, Greece, Portugal, and Cyprus. The obtained results from these case studies showed that the methodology generates accurate data for reducing seismic vulnerability in such buildings [39]. Karic et al. examined historic masonry buildings with brick walls in Vienna, Austria. The

**Table 1**
Material parameters for the numerical model.

| Section | Material | Young modulus (MPa) | | | Type | Poisson ratio | Weight density N/mm$^3$ | Mass density N/mm$^3$/g |
|---|---|---|---|---|---|---|---|---|
| Main building | Hammer-dressed stone walls | 1275 | | | Isotropic | 0.25 | 1.9e-5 | 1.9e-9 |
| | Wooden beams and columns | 9667 (x) | 325 (y) | 325 (y) | Orthotropic | 0.25 | 5e-6 | 5e-10 |
| Minaret | Cut stone walls | 1440 | | | Isotropic | 0.25 | 2e-5 | 2e-9 |
| | Steel Beams | 210000 | | | Isotropic | 0.30 | 7.698e-5 | 7.85e-9 |
| | Roof covered with lead plates | 1400 | | | Isotropic | 0.25 | 1.135e-5 | 1.135e-9 |
| Tomb | Rubble stone walls | 1050 | | | Isotropic | 0.25 | 1.9e-5 | 1.9e-9 |
| | Brick roof | 1650 | | | Isotropic | 0.25 | 1.8e-5 | 1.8e-9 |

considered unique characteristics of the buildings including height and structural regularity/irregularity. They presented comprehensive data on the seismic vulnerability of these buildings [40] Maraveas et al. examined a historic masonry building in Lesbos Island, Greece. Based on the examinations of statically applied load and time history analysis, they determined that the proposed strengthening methods increased seismic performance of the building [41]. Olivito and Porzio developed a new method based on multiple control points for pushover analysis. They tested this method on San Fili Castle of Stignano in Italy. Their results showed that the proposed method yields comprehensive information on the structural behavior and seismic performance of the castle [42].

Although many studies reported on historic buildings, only few studies have examined hypostyle structures. However, it seems that these studies mostly aimed at presenting the historical background of this construction technique in all aspects. Also, architectural features and wooden decorations were examined and these buildings were compared with other buildings with similar architectural styles [43–49]. Some studies, on the hand, examined structural features and construction techniques in addition to the architectural characteristics. In general, previous studies focused on historical context, plan features, or documentation regarding wooden hypostyle mosques [50–54]. On the other hand, only few studies reported seismic performance analysis of a wooden hypostyle structure. Therefore, the current study aimed at presenting a seismic examination of a historic mosque through linear, pushover, and kinematic analyses. Midas Gen [55] and PRO_CINEm [56] programs were used to perform numerical analyses. The results obtained by the linear, pushover, and kinematic analyses were discussed to assess the seismic performance and the local/global failure mechanisms. We believe that our paper contributes to the literature by presenting a comprehensive seismic performance assessment for a historic structure with a rare architectural style.

## 2. Case study: Atabey Gazi Mosque

The mosque was built in 1273 and comprises a main building and a minaret. The mosque sits on a sloped terrain in the southwest of Kastamonu, Turkey (Fig. 1). In similar mosques such as Asian and Arabian hypostyle buildings [57–60]), the span between the pillars was mostly located equally in both directions with a homogeneous distribution in the space, whereas, the central span in *Atabey* mosque is wider than the side spans, resembling a Byzantine basilica-like plan (Fig. 2). Although the name of the mosque is *Atabey Gazi*, it is also called *40 direkli cami* (mosque with 40 pillars). The main building has a rectangular form with dimensions of 30.5 × 19 m. On the northwest of the main building, there is a short minaret with a single balcony, built in the Seljuk style. The mosque is the oldest of the four mosques known to belong to the *Çobanoğulları* period and like the other three mosques, its pillars are wooden and have embroidery decorations [61–65]. However, due to the repairs performed in the past, these architectural characteristics were lost. In the southeast corner of the main building, there is a tomb believed to belong to Atabey Gazi and an additional building between the tomb and the main structure. Nonetheless, these structures were featureless and they were not included in the past restoration work.

### 2.1. Architectural features

There are two entrances to the main building, one from the north and one from the east. The mosque section is 6 stairs down and the *women's gallery* story 9 stairs up. Hexagon imitation bricks were used in slabs; however, in some parts, slabs were covered with mosaic, concrete, and raised wooden flooring. The ceiling was wood-paneled and these panels were supported by transversely and longitudinally placed wooden laths. The doors and windows are also wood. There are iron railings in front of the windows. Interior windows were made of plaster and stained indoor glass windows were used with different patterns. Outer windows were made of concrete and stained glass. The *mihrab* was made of marble in a simple design. The *minbar* (pulpit) was made of stone and has handcrafted stone carvings. The tomb, on the other hand, comprises two separate sections. Rubble and mortar were used in the construction of the main space. Over the rubble stones, 18 × 4 cm bricks were laid with a central pattern. The interior has an octagonal plan, whereas, the outer section in a round form with a dome covered with lead plates. On the north side, there is a section with a small door and wooden floor. Its area is approximately 15 square meters. This section was later built on the empty space between the tomb and the mosque and accesses the mosque through a door. Its walls were built of rubble stone using binder mortar. The ceiling is a wood boat-shaped vaulted roof covered with Marseille tiles.

**Table 2**
Mechanical properties of the masonry walls.

| Definition<br>Masonry unit type | Hammer-dressed stone | Cut stone | Rubble stone | Brick |
|---|---|---|---|---|
| Material type | Isotropic | Isotropic | Isotropic | Isotropic |
| Masonry unit group | Group 1 | Group 1 | Group 1 | Group 1 |
| Unit Volume Weight, kN/m$^3$ | 19 | 20 | 19 | 18 |
| Masonry unit compressive strength, $f_b$ MPa | 5.0 | 5.0 | 5.0 | 5.0 |
| Mortar compressive strength, $f_m$ MPa | 2.5 | 2.5 | 2.5 | 2.5 |
| Characteristic wall compressive strength, $f_k$ MPa | 1.7 | 1.9 | 1.4 | 2.2 |
| Wall initial shear strength, $f_{vko}$ MPa | 0.1 | 0.1 | 0.1 | 0.1 |
| Poisson ratio | 0.25 | 0.25 | 0.25 | 0.25 |
| Wall modulus of elasticity, $E_{wall}$ MPa | 1275 | 1440 | 1050 | 1650 |
| Wall shear modulus, $G_{wall}$ MPa | 510 | 576 | 420 | 660 |

**Table 3**
Plastic material characteristics of the masonry units (for nonlinear analysis).

| Material | Elasticity modulus (MPa) | Poisson's ratio | Tensile strength (MPa) | Stiffness reduction factor |
|---|---|---|---|---|
| Brick | 2000 | 0.25 | 0.20 | 0.00001 |
| Bed joint<br>Head joint | 1250 | 0.25 | 0.15 | 0.00001 |

**Fig. 3.** Degradation, Decay and cracks occurred on the minaret.

### 2.2. Materials

The main walls of the main building are made of rubble stone, but hammer-dressed stones were used in the doorways, the minaret, and around the windows. The *women's gallery* story and carrier columns are wooden. The rubble stone walls on the facades are finished with eaves. The roof cover is wood with Marseille-type tiles. The minaret has a single balcony and is made of hammer-dressed stone.

Properties of the materials used in the numerical model of this mosque complex are shown in Table 1. The macro-modeling method was used in the linear analyses and masonry members and mortar joints are defined as composite materials. Accurate determination of material properties can be a difficult procedure in masonry buildings. Due to some reasons such as difficulty in obtaining required permission from authorities to take samples from historic buildings and structural variability of masonry materials even in different walls, the macro-modeling method was used. The main advantage of the macro-modeling method was low error rate due to the lower number of parameters. Since experimental material tests could not be conducted to determine material properties, the historic data about the structure were reviewed and the materials were selected based on this information and the parameters given in TBEC (2018) [67] and SRMGHS 2017'de [68]. According to TBEC (2018), the elastic modulus of the wall ($E_{wall}$) should be 750 times the characteristic wall compressive strength ($f_k$); on the other hand, wall shear modulus ($G_{wall}$) should be 40% of the elastic modulus of the wall. Class GL24h materials were used in the wooden beams and columns of the main building, and S235 steel was used for steel beams of the minaret. The parameters defined for masonry walls are given in Table 2. Furthermore, the parameters used in the nonlinear analysis of the masonry members and mortar joints are shown in Table 3. The simplified micro-modeling method was used in the nonlinear analysis. This method is based on the assumption that masonry units are separated by thin mortar joints. Therefore, the mechanical properties of the masonry wall members, masonry units and mortar joints, were separately defined into the model.

### 2.3. Physical deteriorations

Physical deteriorations formed on the outer walls of the main building over time. Particularly, the west and north facades were

**Table 4**
Work performed during the restoration.

| Place | Description |
|---|---|
| Pillars | The 25 × 25 sized pillars added to both sides of the entrance door during the past interventions were removed and the number of total pillars inside the mosque was rearranged to be 40 (as in the original architecture). |
| Roofing | After the later-added pillars were removed, the roof's carrier system was restructured. The Marseille-type tile cover was removed, the damaged parts of the wooden cover were repaired and covered with lead plates. |
| Women's gallery | To merge the women's galleries on both sides of the mosque, the women's gallery story, which was shifted with the later-added pillars, was removed. |
| Rooms/doors | The rooms created by dividing with windows on both sides of the entrance door and the glass door that was built directly opposite the main entrance door were removed. |
| Annex building | The annex building that was later added between the tomb and the mosque was removed; the tomb was renewed. The slabs were improved, the octagonal form in the inner part and the cylindrical form in the outer part was re-achieved. The entire exterior brick cladding was renewed, the dome was completed and was covered with lead plates. |
| Minaret | The minaret was dismantled up to the balcony and was rebuilt together with the slabs and balustrades. The cone part is covered with lead. The deteriorated stones in the entire minaret were renewed. |
| Main exterior walls | Cement joints on the body walls were cleaned, deteriorated and rotten stones were renewed and Khorasan-style joints were made. Window chimneys were renewed with the same-sized stones. |
| Slabs of women's gallery | Sagging and deflections in some parts of the slabs of the *women's gallery* were removed; its carrier system, wooden cover and underfloor ceiling covering were renewed. |
| Eaves | All of the eaves on the south facade were removed, the deteriorations in the eave level were corrected, and these parts were rebuilt. |
| Slabs | During the restoration, excavations were carried out in the mosque for research purposes, imitation brick slabs and concrete slabs were removed, and wooden slabs were placed at the original slab level. |
| Scraper | The existing interior plasters were scraped, Khorasan-style plaster was applied and painted. |
| Window/ iron grills | On the east side of the mosque, windows that were closed for various reasons and turned into doors for passage to the tomb were opened, and wooden frames and iron grills were added. |
| Window/ iron grills | On the west side of the mosque, the ground level around the windows, which were closed by filling (since the ground level increased over time and therefore remained below ground level) was partially lowered and the windows were re-opened. Wooden frames and iron grills were added. |
| Interior /outdoor stained glass windows | Deteriorated plaster interior windows were replaced based on the details specified in the building survey. All of the concrete outdoor were renewed. |
| Window/ iron grills | All wooden frames and iron grills were renewed in accordance with the original architecture |

buried underground. Two windows and one door on the *women's gallery* story of the west facade were filled and closed since they were below the surface level. One window on the ground floor of the west facade was closed by laying up bricks. Some of the windows on the wall connecting the tomb and the main building were partially closed, some were demolished, and a door to the tomb was built. Since the main walls of the western facade were affected by rainwater, the soil around the facade walls was opened up to the ground floor level and a 30 m long and 2.5 m high covered water drainage culvert was placed under the road. Although the door and window frames were renovated in the past, there are still deteriorations. No excessive deterioration or collapse was observed in the wooden roof. However, deteriorations and deflections were observed in the slabs of the *women's gallery*. Excessive degradation and decay occurred on the stone base of the minaret and there are vertical hair cracks especially on the balcony story and parapet stones (Fig. 3). Furthermore, cracks are detected in the stone handrails of the balcony [69]. There are also collapses in the wooden structured cone section of the lead-coated minaret.

The most deteriorated part of the structure is the brick main body walls of the tomb. Some interventions were made to this section in the past and the pattern and design on the exterior walls of the tomb have lost. There were collapses and deteriorations in the saddle roof of the tomb. There are also ruptures, sagging, and deformations in the lower wooden coverings of the roof, and therefore the bearing elements of the roof came out. There are also partial deteriorations in the lead coating plates and the carrier wooden structure in the dome of the tomb. In the whole of the tomb, there was deterioration and sagging on the wooden slabs that would pose a safety hazard.

### *2.4. Interventions*

The main structure of the mosque has undergone various repairs in the past that changed its original architecture [70]. The oldest repair was made in 1568 by the order of Suleiman the Magnificent. The structure was later repaired in 1705. We thought that top windows were added during these repairs since these windows are seen in the structures of that periods. Therefore, it seems that the mosque complex had undergone significant repairs in 1568 and 1705. Also, at the entrance of the building, there are inscriptions belonging to the repairs dated 1800 and 1871. It is thought that the additional building between the tomb and the main structure, which clearly represents the influence of the Westernization period, was built during these repairs [71]. Moreover, it is believed that the porch in front of the main entrance was built during this period. This mosque, where local/social activities were held in 1922, was recognized as the city's temple in the best condition. The mosque has also undergone some interventions during the Republican period. After the 1943 earthquake, known as the great earthquake, the lead plates on the roof were removed and used in other mosques. The roof of the mosque was then covered with Marseille tiles. The mosque has later undergone some minor repairs and wooden eaves were added in front of the entrance door on the side.


**Fig. 4.** Post-restoration images of the mosque. (a-c) Two entrances of the mosque (d) Interior of the mosque.

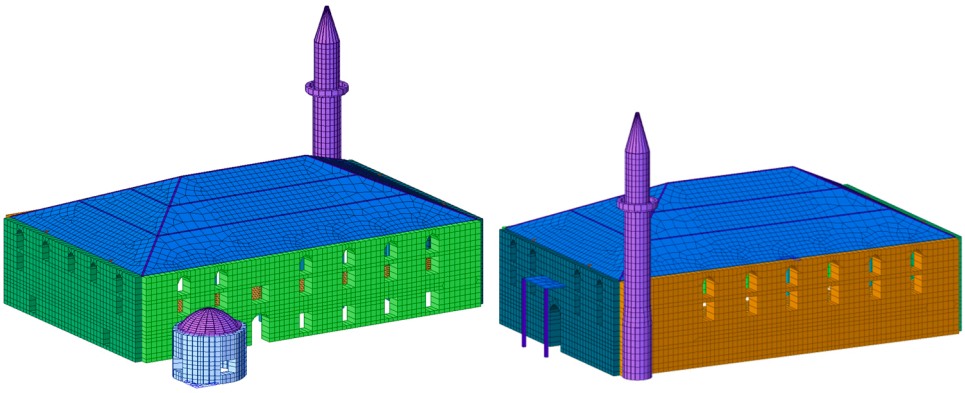

**Fig. 5.** Finite element model of the mosque (main section, minaret and tomb). Front (left) and back (right) views.

## 3. Restoration stage

As discussed above, this 750-year-old mosque has undergone many interventions in the past. The restoration project was aimed to bring back the building to its original form and to correct the structural deteriorations and deformations in the materials inside and outside the mosque, considering the information and evidence stated in the completely reliable source document. Accordingly, a comprehensive restoration was performed in 2009. The work performed during the restoration is presented in Table 4. Post-restoration images of the mosque are shown in Fig. 4.

## 4. Numerical approach

A finite element model of this masonry mosque complex comprising the main building, a minaret, and a tomb, was prepared using MIDAS Gen [55] software. Linear and nonlinear analyses were performed on this finite element model. The front and back views of the finite element model of the mosque complex are given in Fig. 5.

To determine the modes of the structure, a modal analysis was performed using the Ritz vector method. For response spectrum analysis, on the other hand, equivalent earthquake loading was used. In accordance with the TBEC 2018 code [67], base shear forces calculated for the earthquake loadings in the x and y directions were increased to 80% of the base shear force corresponding to the equivalent earthquake loads while applying equivalent earthquake loading to the structure. Earthquake levels described in the TBEC

**Table 5**
Earthquake classes.

| Earthquake class | Definition |
|---|---|
| DD1 | *Most extensive earthquake class* having a 2% 50-year exceedance probability with a mean return period of 2475. |
| DD2 | *Standard design earthquake class* having a 10% 50-year exceedance probability with a mean return period of 475 years. |
| DD3 | *Frequent* earthquake class having a 50% 50-year exceedance probability with a mean return period of 72 years. |

**Table 6**
Parameters used in the seismic performance analyses.

| **Parameters** | **Value / Class** |
|---|---|
| Earthquake class and corresponding performance level | Limited damage for DD3<br>Controlled damage for DD2 |
| Analysis method | Linear |
| Story drift limits | 0.3% for limited damage<br>0.7% for controlled damage |
| Seismic load reduction factor, Ra | Ra= 1 for DD3<br>Ra= 3 for DD2 |

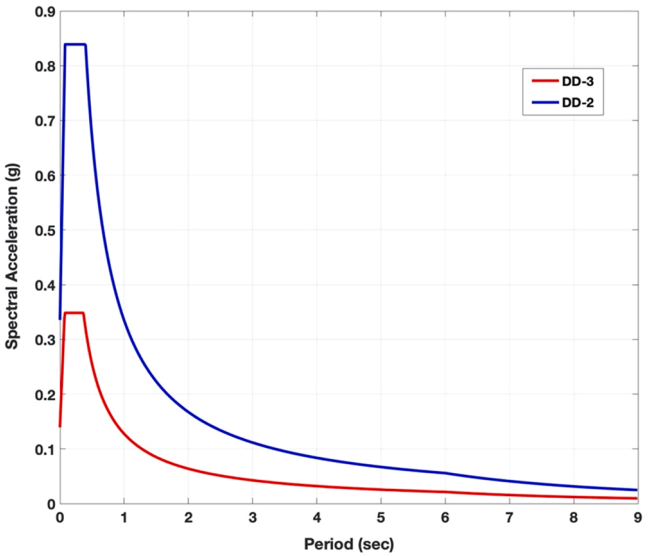


**Fig. 6.** Elastic spectrum for different ground motion levels, (Ra=1).

2018 code are given in Table 5.

Linear seismic performance analysis was conducted for the mosque. This analysis approach assumes that the building exhibits linear elastic behavior under seismic loads. Since window edges in masonry walls are critical points, these members were defined as critical sections in the finite element model and shear forces were evaluated considering these members. In seismic analyses, DD3 and DD2 earthquake levels with a 50% and 10% chance of being exceeded in 50 years were considered, respectively. Furthermore, the fact that the mosque has national importance was taken into account in the analyses in accordance with the SRMGHS 2017 [68]. This guide requires consideration of DD3 and DD2 earthquake levels in the analyses and evaluations of structures with national importance. Accordingly, such buildings are expected to satisfy the Limited Damage performance level for a DD3 earthquake and Controlled Damage performance level for a DD2 earthquake, respectively. The information level about the structure was accepted as "limited" and the building information coefficient was taken as 0.75 in the calculations. Performance limits considered in the analyses are given in Table 6.

The TBEC 2018 code suggests using earthquake spectra obtained from Earthquake Hazard Map [72]. After determining the location of the building on the map, the required earthquake parameters for the elastic spectrum curve were obtained using soil class and the earthquake level. Since the soil class of the terrain, where the examined mosque exists, was found to be ZC, seismic analyses of the structure were conducted for DD3 and DD2 earthquakes according to the SRMGHS 2017 [68] guide. The spectral acceleration coefficients ($S_{DS}$, $S_{D1}$) corresponding to these ground motion levels were calculated using Eq. 1 and Eq. 2.

For a DD3 class earthquake:

**Table 7**
Soil and earthquake variables.

| Parameters | Value / Class |
|---|---|
| Local soil class | ZC |
| Earthquake class | DD3, DD2, DD1 |
| Earthquake map spectral acceleration coefficients | DD3, $S_s = 0.268$, $S_1 = 0.085$<br>DD2, $S_s = 0.648$, $S_1 = 0.223$ |
| Peak ground acceleration | DD3, PGA = 0.116<br>DD2, PGA = 0.289 |
| Local soil effect coefficients | DD3, $F_s = 1.300$, $F_1 = 1.500$<br>DD2, $F_s = 1.226$, $F_1 = 1.500$ |
| Spectral acceleration coefficients | DD3, $S_{DS} = 0.348$, $S_{D1} = 0.127$<br>DD2, $S_{DS} = 0.839$, $S_{D1} = 0.335$ |
| Live load participation coefficient (n) | 0.60 |

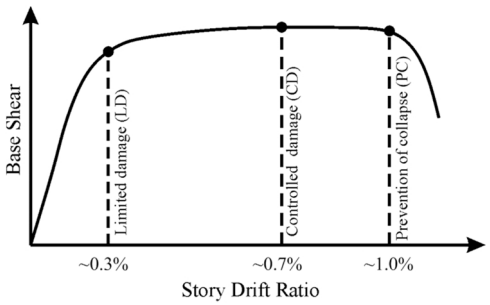


**Fig. 7.** Pushover curve and limit states [68].

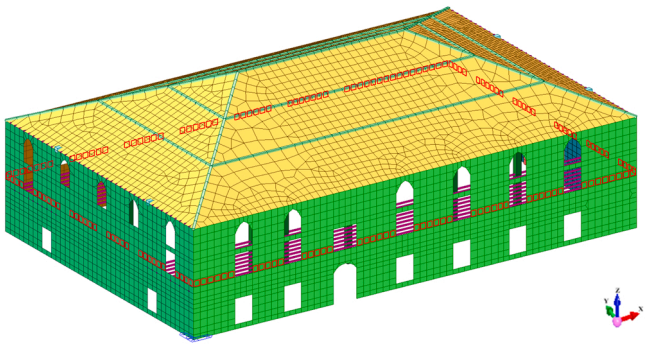

**Fig. 8.** Critical sections of the masonry walls (red-colored parts).

$$S_{DS} = S_S \times F_S = 0.268 \times 1.300 = 0.348 S_{D1} = S_1 \times F_1 = 0.085 \times 1.500 = 0.127 \quad (1)$$

For a DD2 class earthquake:

$$S_{DS} = S_S \times F_S = 0.684 \times 1.226 = 0.839 S_{D1} = S_1 \times F_1 = 0.223 \times 1.500 = 0.335 \quad (2)$$

Where $S_s$ and $S_1$ are spectral acceleration coefficients; $F_s$ and $F_1$ are ground effect coefficients for short period and 1-sec period, respectively. Elastic spectrum curves obtained for DD3, DD2, and DD1 earthquakes considering seismic load reduction factor (Ra) as 1 are given in Fig. 6. The soil class and earthquake parameters used in the numerical analyses are listed in Table 7.

For static pushover analysis of historic structures, the SRMGHS 2017 [68] assumes three different performance levels. Limit states corresponding to these performance levels are shown in Fig. 11. According to the curve considering inter-story drifts and base shear forces, inter-story drift ratio limits corresponding to the limited damage, controlled damage, and pre-collapse damage levels are 0.3%, 0.7%, and 1.0%, respectively (Fig. 7). Plastic material characteristics used in the nonlinear analysis are presented in Table 3.

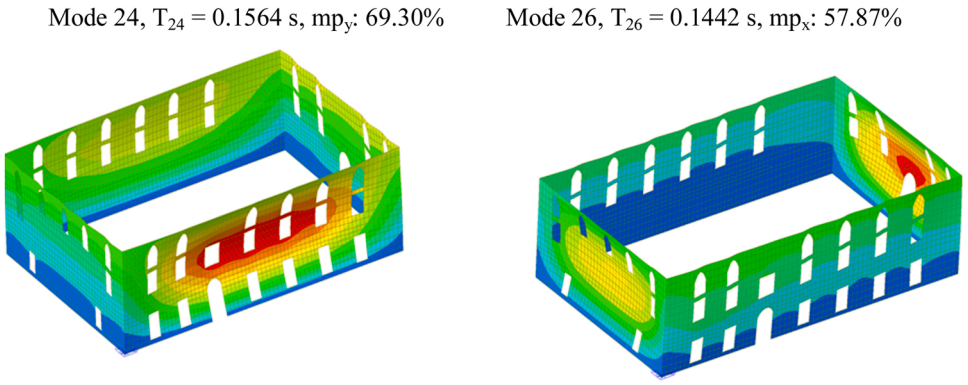


**Fig. 9.** Mod shapes ($mp_x$ and $mp_y$: mass participation for x and y directions).

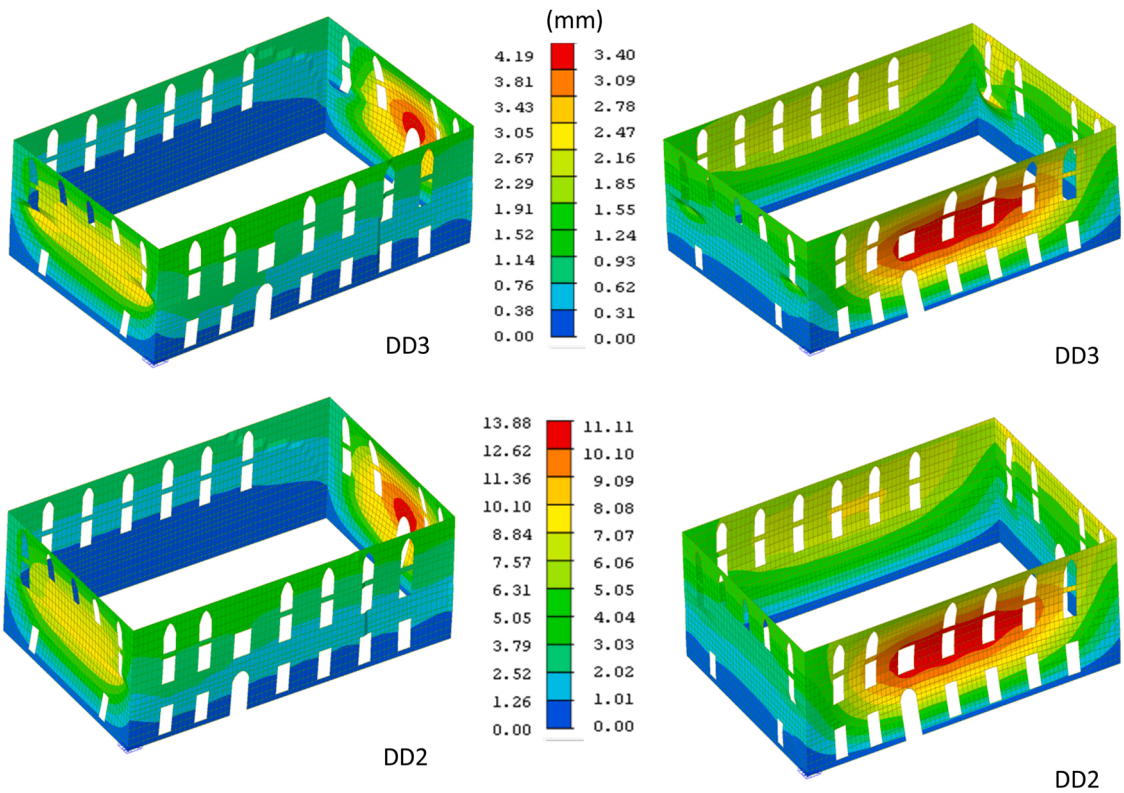


**Fig. 10.** Lateral displacements of the structure under earthquake effects: D+L+Exp (left), D+L+Eyp (right) (Exp and Eyp are earthquake forces in the positive x and y directions, respectively).

**Table 8**
Inter-Story Drift Examinations.

| Earthquake class | Displacement ΔD, (mm) | | Drift ratio, ΔD/H | | Limit | Check |
|---|---|---|---|---|---|---|
| | x | y | % | % | % | √ / × |
| DD3 | 1.1 | 1.7 | 0.015 | 0.023 | 0.3 (LD) | √ |
| DD2 | 3.8 | 5.5 | 0.052 | 0.077 | 0.7 (CD) | √ |

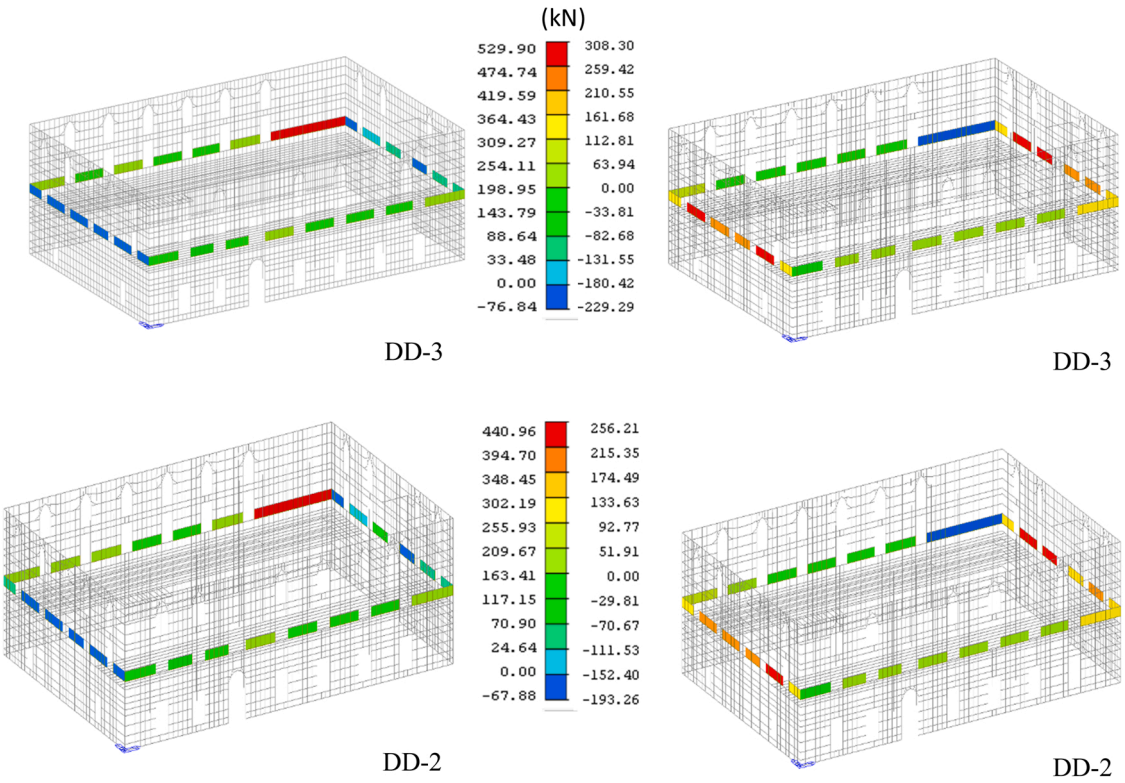


**Fig. 11.** Shear forces under seismic effects: D+L+Exp (left), D+L+Eyp (right) (Exp and Eyp are earthquake forces in the positive x and y directions, respectively).

**Table 9**
Performance analysis.

| Earthquake class | Ra | Shear force checking | * % r | Target performance | Check |
|---|---|---|---|---|---|
| DD3 | 1 * * | √ | 0 | LD | √ |
| DD2 | 3 * * | √ | 11.1 | CD | √ |

*The ratios of the shear forces on the masonry walls failed in shear to the total shear force acting on the same story. * *According to SRMGHS 2017 guide.

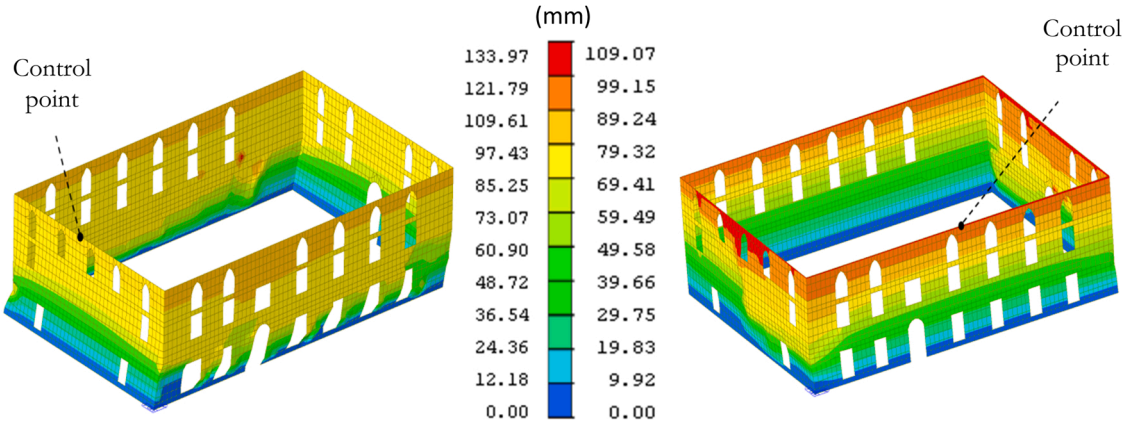


**Fig. 12.** Selected control points for positive x and y directions (left: x, right: y direction).

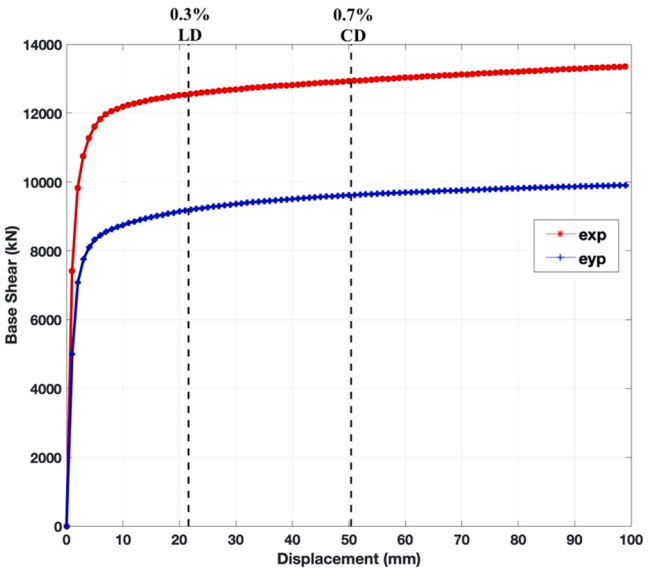


**Fig. 13.** Base shear vs. displacement.

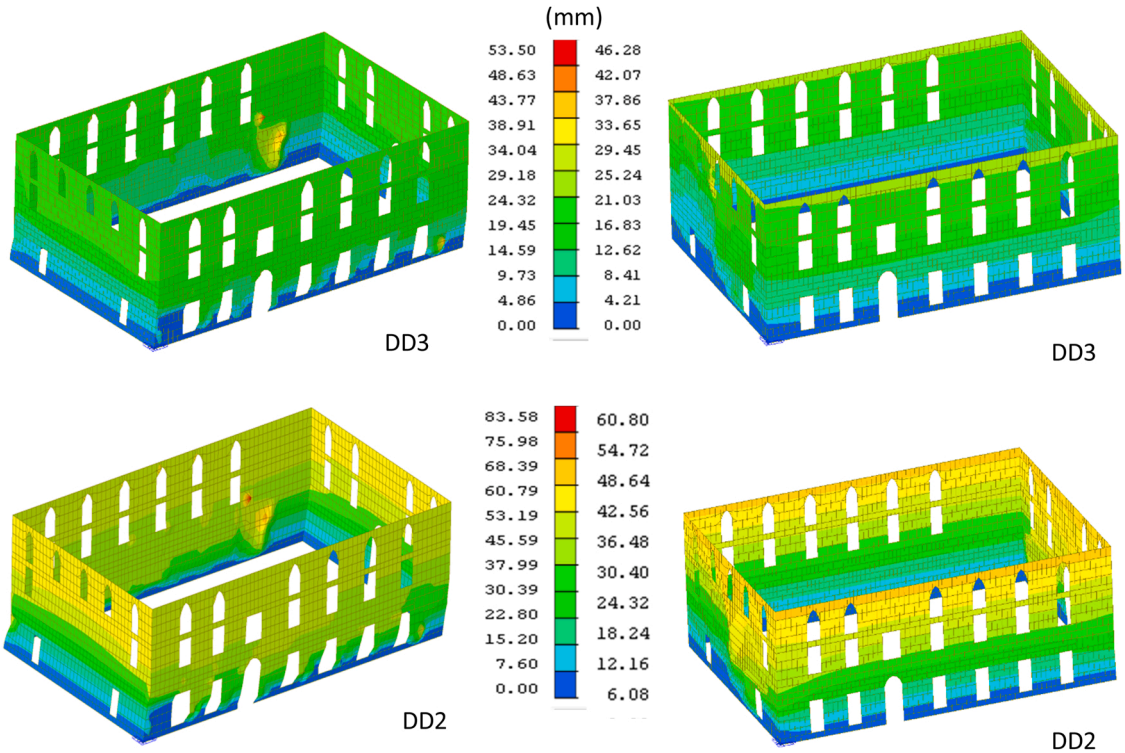


**Fig. 14.** Lateral displacements under seismic effects: D+L+Exp (left), D+L+Eyp (right) (Exp and Eyp are earthquake forces in the positive x and y directions, respectively).

### *4.1. Main section of the mosque*

#### *4.1.1. Linear analysis*

Critical sections selected along the window level of the main building are shown in Fig. 8. Material characteristics used in the numerical modeling are given in Table 2. Two mode shapes with the highest mass participation factors determined by modal analysis are shown in Fig. 9.

**Table 10**
Displacement checks for control points.

| Earthquake Class | Base shear (kN) | | Performance point (mm) | | Drift ratio | | Limit ratio | Check |
|---|---|---|---|---|---|---|---|---|
| | x | y | xp | yp | % | % | % | √ / × |
| DD3 | 12534 | 9165 | 20.9 | 21.0 | 0.291 | 0.292 | 0.3 (LD) | √ |
| DD2 | 12926 | 9613 | 50.0 | 50.0 | 0.694 | 0.695 | 0.7 (CD) | √ |

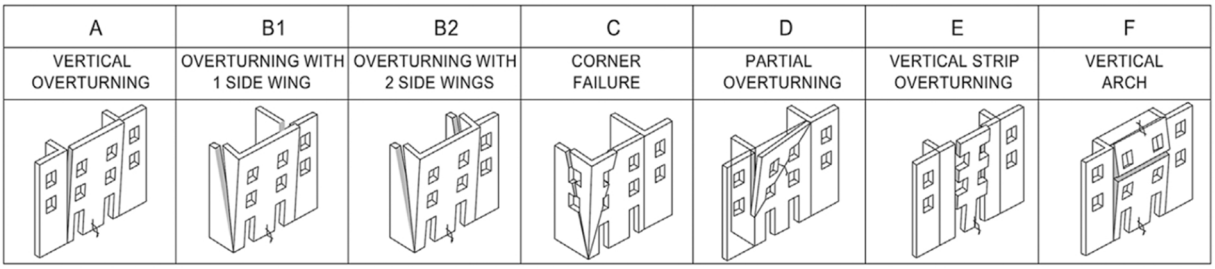


**Fig. 15.** Out-of-plane collapse behaviors of the masonry walls [73].

**Table 11**
Kinematic analysis parameters.

| Earthquake Class | PGA | $S_{DS}$ | $R_a$ | $a_g$ |
|---|---|---|---|---|
| DD3 | 0.116 | 0.348 | 1 | 0.040 g |
| DD2 | 0.289 | 0.839 | 2 | 0.121 g |

The displacements observed in the main building under seismic loadings in the x and y directions for two earthquake classes are given in Fig. 10. These results indicated that the building satisfies "Limited Damage" and "Controlled Damage" performance target for DD3 and DD2 class earthquakes, respectively (Table 8).

Considering the vertical and earthquake loads together, the current condition of this mosque was found to satisfy the "limited damage" and "controlled damage" performance criteria for shear forces under DD3 and DD2 earthquake levels, respectively. Shear forces on the critical sections of the masonry walls generated by the earthquake forces in the positive x and y directions are shown in Fig. 11. The shear force evaluation for masonry walls in accordance with the SRMGHS 2017 [68] guide is given in Table 9.

*4.1.2. Nonlinear analysis*

Considering the pre-collapse performance criteria assuming an inter-story drift ratio of 1%, static pushover forces were applied until a displacement of 100 mm -which corresponds to a higher value of %1 of the building height, 72 mm- was achieved. Nonlinear analyses were performed for the positive x and y directions separately. The control points selected from the top of the building are shown in Fig. 12.

The displacement curve for base shear forces in the positive x and y directions is given in Fig. 13. Lateral load capacities were found to be 13136 and 9771 kN for earthquake forces in the positive x and y directions, respectively. Vertical dashed lines in the graph indicate the displacement limits for Limited Damage and Controlled Damage performance criteria. The displacements that occurred with the pushover analysis are shown in Fig. 14.

According to the inter-story drifts obtained by the pushover analysis, the building was found to satisfy Limited Damage and Controlled Damage performance target for DD3 and DD2 ground motion levels, respectively.

Displacements obtained at the 21st and 50th pushover steps for DD3 and DD2 earthquakes are given in Table 10, respectively. These pushover steps correspond to the inter-story drift limits of 0.3% and 0.7% for DD3 and DD2 earthquakes, respectively.

*4.1.3. Kinematic analysis*

Inadequate connection between the masonry walls and slabs limits rigid diaphragm behaviors and causes local displacements on the walls. Therefore, kinematic analysis which provides information about local behaviors of masonry buildings under seismic loading is important. The out-of-plane collapse behaviors of the masonry walls under earthquake loads are given in Fig. 15.

To examine local behaviors on the walls of the main building, three mechanisms, namely, lateral bending, vertical bending, and overturning were considered. To observe these behaviors, kinematic analysis was conducted using Pro_CINEm software [56]. Like linear and nonlinear analyses, two different ground motion levels were considered in the kinematic analysis. Peak ground accelerations

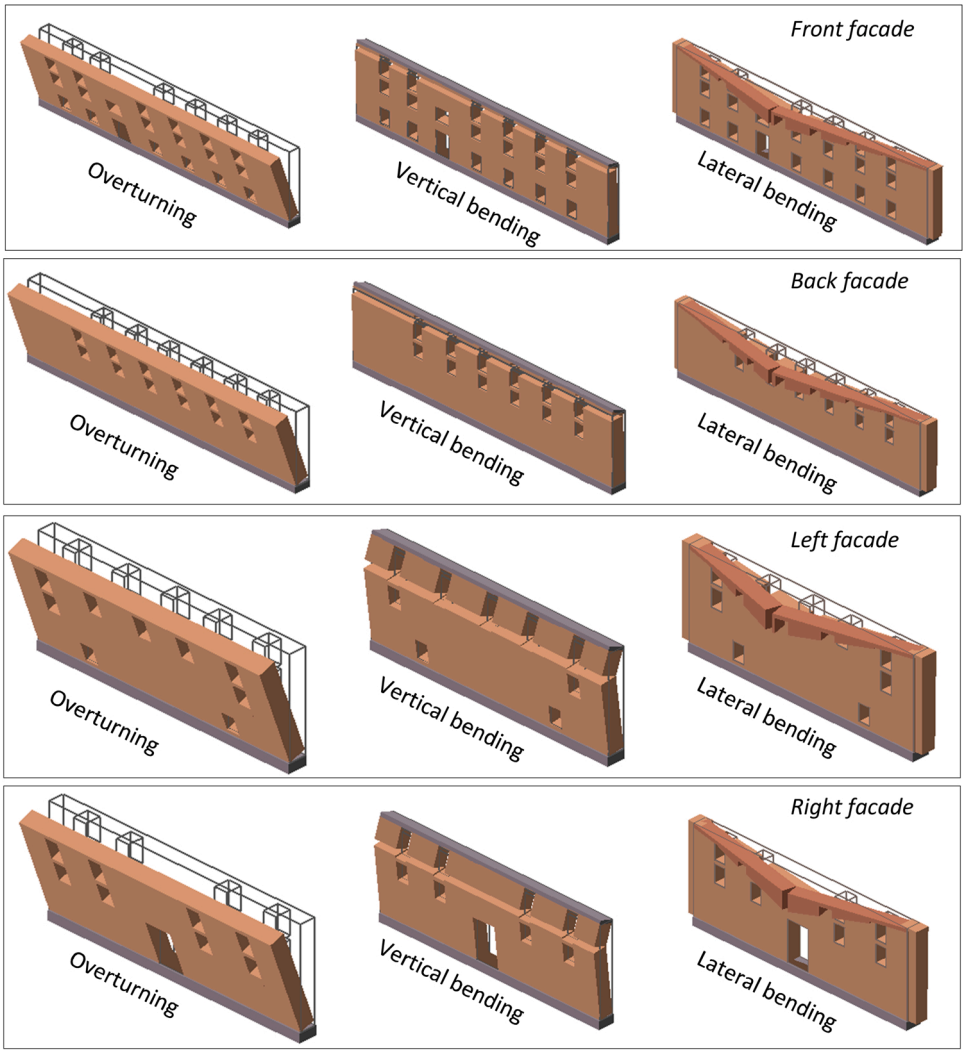


**Fig. 16.** Mechanisms observed for all facades.

($a_g$) were calculated as 0.166 g and 0.289 g; $S_{DS}$ values as 0.348 and 0.839 for DD3 and DD2 earthquake levels, respectively. According to the SRMGHS 2017 [68], seismic load reduction factors were taken as Ra= 1 and Ra= 2. While evaluating the analysis results, an $a_c/a_0$* value $\leq 1$ indicates that the related mechanism occurs; whereas, an $a_c/a_0$* value $> 1$ means the related mechanism does not occur. The parameters used in the kinematic analysis were listed in Table 11. The collapse mechanisms observed for all facade walls are shown in Fig. 16. The results of the kinematic analysis are given in Table 12.

As seen in Table 13, the evaluation of the walls indicated that the walls, in general, did not have sufficient strength against lateral bending, vertical bending, and overturning mechanisms. Although the kinematic analysis results revealed that overturning and bending mechanisms occurred on the main building, we concluded that the mechanisms observed will not pose a safety risk in a possible earthquake since the exterior walls are bonded with cramp iron.

### 4.2. Minaret of the mosque

#### 4.2.1. Linear analysis

The minaret is a part of this mosque complex and consists of masonry walls, steel beams, and a roof covered with lead plates. The finite element model of the minaret, critical sections, and the first four modes are shown in Fig. 17. The material properties used in the modeling of the minaret are listed in Table 2.

The displacements observed in the minaret under seismic loadings in the x and y directions for two earthquake classes are given in Fig. 18. These results showed that the minaret meets "Limited Damage" and "Controlled Damage" performance target for DD3 and DD2 ground motions, respectively (Table 14).

Considering the vertical and earthquake loads together, we found that the current condition of the minaret satisfies the "Limited

**Table 12**
Kinematic analysis results for all (four) facades.

| | Mechanism* | Earthquake class | $\alpha_0$ | $a_0^*$ (g) | $a_c$ (g) | $a_c/a_0^*$ | Check ($a_c/a_0^*$) |
|---|---|---|---|---|---|---|---|
| Front facade | 1 | DD3 | 0.144 | 0.111 | 0.040 | 0.360 | × |
| | | DD2 | 0.144 | 0.111 | 0.121 | 1.090 | √ |
| | 2 | DD3 | 0.383 | 0.284 | 0.040 | 0.141 | × |
| | | DD2 | 0.383 | 0.284 | 0.121 | 0.426 | × |
| | 3 | DD3 | 0.129 | 0.097 | 0.080 | 0.825 | × |
| | | DD2 | 0.129 | 0.097 | 0.121 | 1.247 | √ |
| Back facade | 1 | DD3 | 0.184 | 0.141 | 0.040 | 0.283 | × |
| | | DD2 | 0.184 | 0.141 | 0.121 | 0.858 | × |
| | 2 | DD3 | 0.452 | 0.335 | 0.040 | 0.119 | × |
| | | DD2 | 0.452 | 0.335 | 0.121 | 0.361 | × |
| | 3 | DD3 | 0.166 | 0.124 | 0.080 | 0.645 | × |
| | | DD2 | 0.166 | 0.124 | 0.121 | 0.975 | × |
| Left facade | 1 | DD3 | 0.140 | 0.116 | 0.040 | 0.344 | × |
| | | DD2 | 0.140 | 0.116 | 0.121 | 1.043 | √ |
| | 2 | DD3 | 0.683 | 0.506 | 0.040 | 0.079 | × |
| | | DD2 | 0.683 | 0.506 | 0.121 | 0.239 | × |
| | 3 | DD3 | 0.104 | 0.078 | 0.080 | 1.025 | √ |
| | | DD2 | 0.104 | 0.078 | 0.121 | 1.551 | √ |
| Right facade | 1 | DD3 | 0.121 | 0.100 | 0.040 | 0.400 | × |
| | | DD2 | 0.121 | 0.100 | 0.121 | 1.210 | √ |
| | 2 | DD3 | 0.663 | 0.491 | 0.040 | 0.081 | × |
| | | DD2 | 0.663 | 0.491 | 0.121 | 0.246 | × |
| | 3 | DD3 | 0.121 | 0.092 | 0.080 | 0.869 | × |
| | | DD2 | 0.121 | 0.092 | 0.121 | 1.315 | √ |

* 1: Overturning, 2: Vertical bending, 3: Lateral bending

**Table 13**
Results of the kinematic analysis.

| | Mechanism control ($a_c/a_0^*$) | | |
|---|---|---|---|
| Earthquake class | 1 | 2 | 3 |
| DD3 | × | × | × |
| DD2 | × | × | × |

* 1: Overturning, 2: Vertical bending, 3: Lateral bending

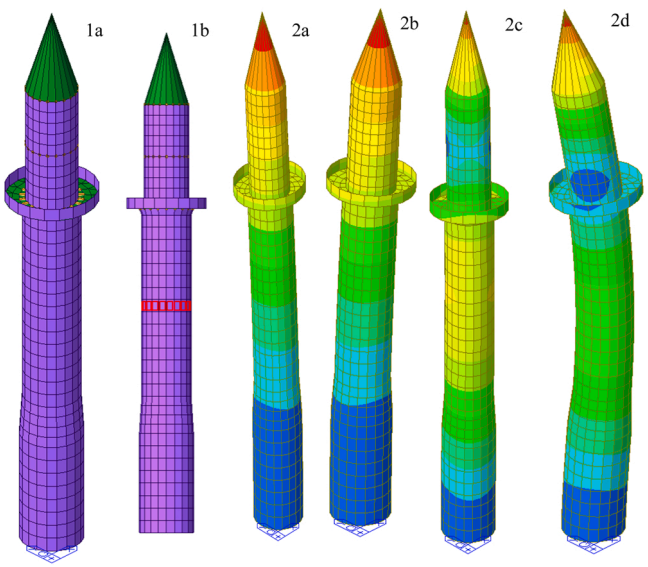


**Fig. 17.** Finite element model of the minaret (1a), Critical masonry walls (red-colored parts) (1b), Four modes (2a=0.9286, 2b=0.9286, 2c=0.1677, 2d=0.1677 s).

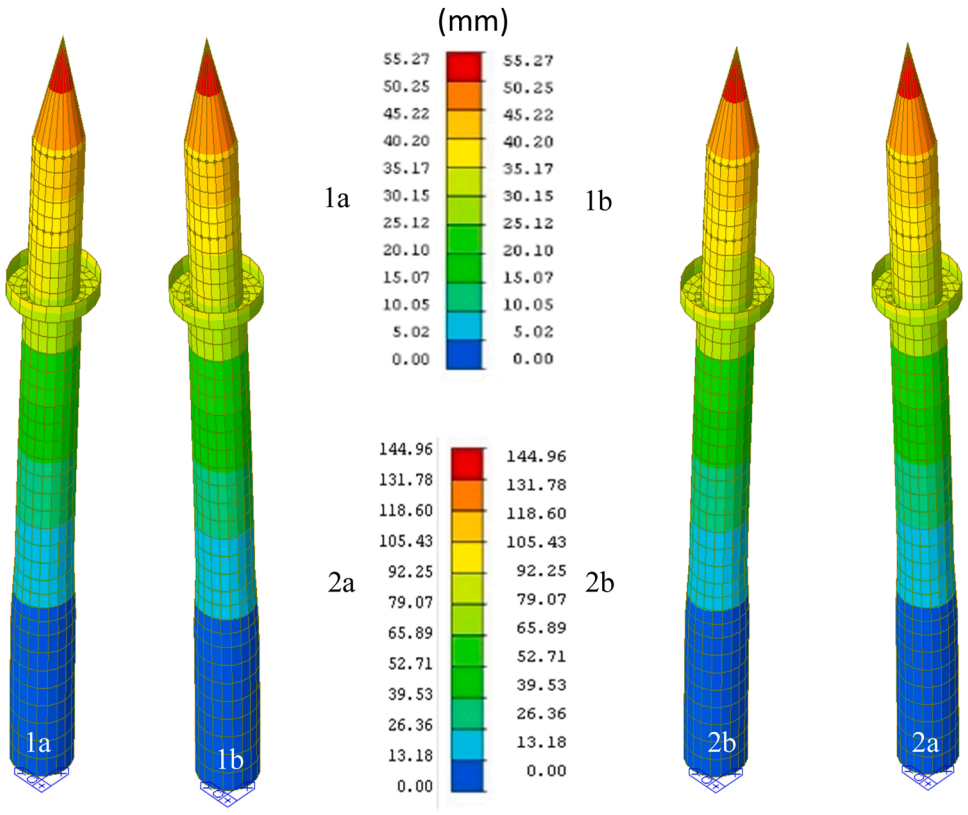


**Fig. 18.** Displacements observed in the minaret (1a:DD3 Exp, 1b:DD3 Eyp, 2a:DD2 Exp, 2b:DD2 Eyp).

**Table 14**
Relative floor displacement controls for the minaret.

| Earthquake level | Displacement ΔD, (mm) | | Drift ratio, ΔD/H | | Limit | Check |
|---|---|---|---|---|---|---|
| | x | y | % | % | % | √ / × |
| DD3 | 44.6 | 44.6 | 0.258 | 0.258 | 0.3 (LD) | √ |
| DD2 | 117.0 | 117.0 | 0.678 | 0.678 | 0.7 (CD) | √ |

Damage" and "Controlled Damage" performance criteria for shear forces under DD3 and DD2 earthquake levels, respectively. Shear forces on the critical sections of the masonry walls caused by the earthquake forces are given in Fig. 19. Shear force checks for masonry walls in accordance with the SRMGHS 2017 [68] guide are presented in Table 15.

*4.2.2. Nonlinear analysis*

Considering the pre-collapse performance criteria assuming an inter-story drift ratio of 1%, static pushover forces were applied until a displacement of 200 mm –which corresponds to a higher value of %1 of the minaret height (172.6 mm)– was achieved. Nonlinear analyses were performed for the positive x and y directions separately. The control points selected from the top of the minaret are shown in Fig. 20.

The displacement curve for base shear forces in the positive x and y directions is given in Fig. 21. The lateral load capacity of the minaret was found to be 38.3 kN for both earthquake forces in the positive x and y directions. Vertical dashed lines in the graph indicate the displacement limits for Limited Damage and Controlled Damage performance criteria. The displacements observed on the minaret by the pushover analysis are shown in Fig. 24.

According to the inter-story drift values obtained with the pushover analysis, the minaret was found to have satisfactory strength for the "limited damage" and "controlled damage" performance criteria under DD3 and DD2 earthquake levels, respectively. Fig. 22.

The displacement results obtained at the 51st and 120th pushover steps for DD3 and DD2 class earthquakes are shown in Table 16. These pushover steps correspond to the inter-story drift limits of 0.3% and 0.7% for DD3 and DD2 ground motions, respectively.

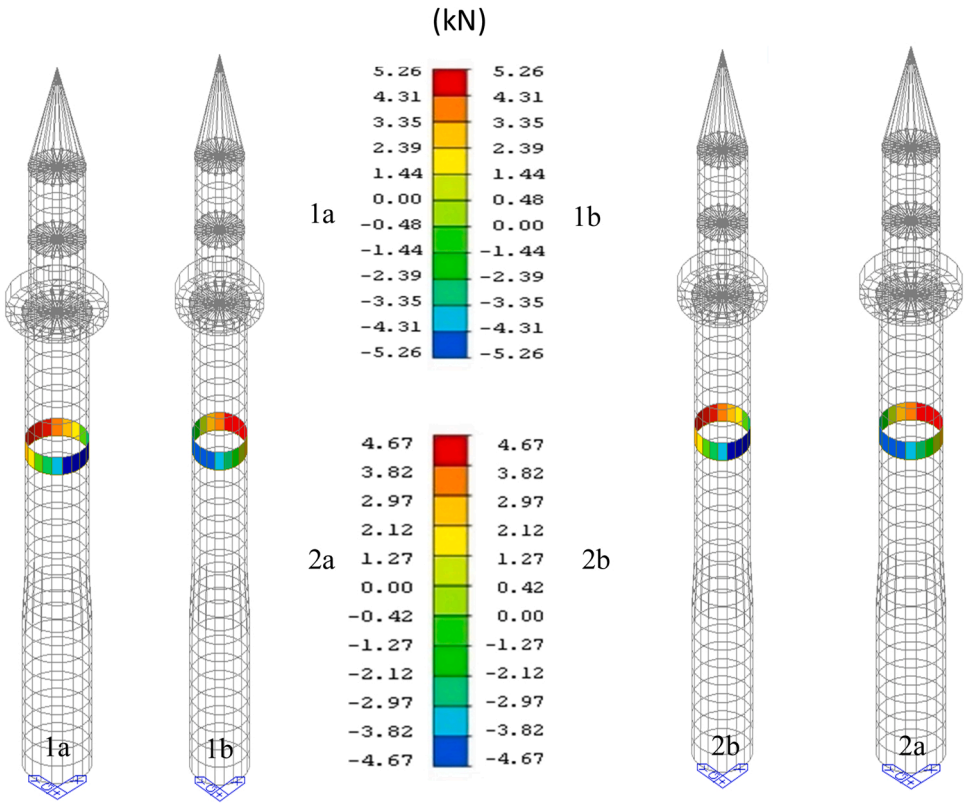


**Fig. 19.** Shear forces on the minaret (1a:DD3 Exp, 1b:DD3 Eyp, 2a:DD2 Exp, 2b:DD2 Eyp).

**Table 15**
Seismic performance evaluation results.

| Earthquake class | Ra | Shear force checking | * % r | Target performance level | Checking |
|---|---|---|---|---|---|
| DD3 | 1 * * | √ | 0 | LD | √ |
| DD2 | 3 * * | √ | 0 | CD | √ |

*The ratios of the shear forces on the masonry walls failed in shear to the total shear force acting on the same story. * * According to the SRMGHS 2017.

### 4.3. The tomb

#### 4.3.1. Linear analysis

Critical sections of the tomb were selected along the window axis as shown in Fig. 23 (red lines). Material properties defined in the FE model of the tomb are listed in Table 2. Mod shapes of the tomb obtained by modal analysis under vertical loads are given in Fig. 24.

The displacements observed in the tomb under earthquake loadings in the x and y directions for two earthquake classes are given in Fig. 25. The displacement results revealed that the tomb satisfies the “Limited Damage” and “Controlled Damage” performance criteria for DD3 and DD2 earthquakes, respectively (Table 17).

Considering the vertical and earthquake loads together, we determined that the current condition of the tomb meets the “limited damage” and “controlled damage” performance target for shear forces under DD3 and DD2 earthquake levels, respectively. Shear forces on the critical sections of the masonry walls caused by the earthquake forces are given in Fig. 26. Shear force checks for masonry walls in accordance with the SRMGHS 2017 [68] guide are presented in Table 18.

#### 4.3.2. Nonlinear analysis

Considering the pre-collapse performance criteria assuming an inter-story drift ratio of 1%, static pushover forces were applied until a displacement of 60 mm, which corresponding to a higher value of %1 of the tomb height (40 mm) was achieved. Nonlinear analyses were performed for the positive x and y directions separately. The control points selected from the top of the tomb are shown in Fig. 27.

The displacement curve for base shear forces in the positive x and y directions is given in Fig. 28. The lateral load capacities of the

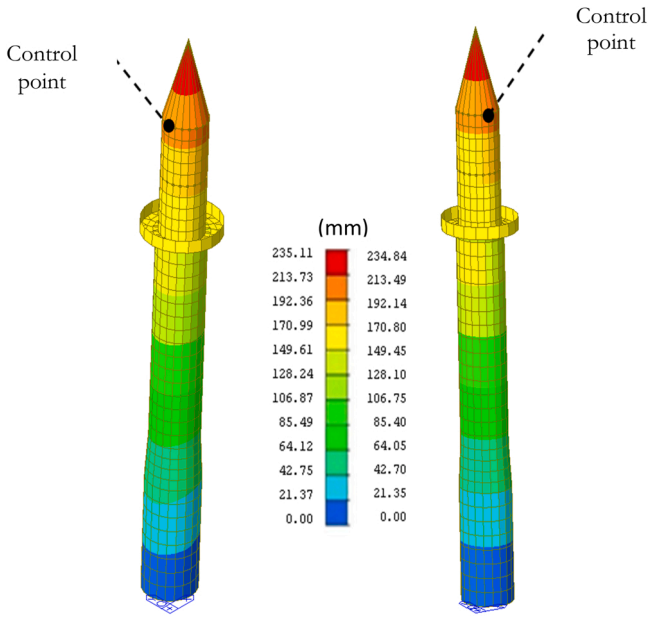


**Fig. 20.** Control points of the minaret for earthquake loads in the positive x (left) and y (right) directions.

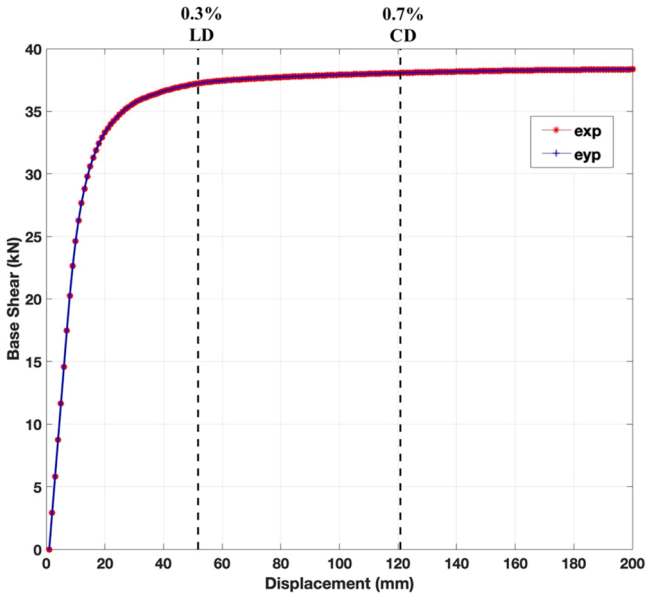


**Fig. 21.** Base shear vs. displacement.

tomb were calculated as 846 kN and 883 kN for earthquake forces in the positive x and y directions, respectively. Vertical dashed lines in the graph indicate the displacement limits for Limited Damage and Controlled Damage performance levels. The displacements observed on the tomb by the pushover analysis are shown in Fig. 29.

According to the inter-story drift values obtained with the pushover analysis, we found that the tomb has satisfactory strength for the "Limited Damage" and "Controlled Damage" performance levels for DD3 and DD2 earthquake levels, respectively.

The displacement results obtained at the 11th and 27th pushover steps for DD3 and DD2 earthquakes are shown in Table 19, respectively. These pushover steps correspond to the inter-story drift limits of 0.3% and 0.7% for DD3 and DD2 earthquakes, respectively.

This Mosque Complex was built in 1273 and has deep historic roots. The tomb building is a separate structure. Plus, since the minaret is higher than the main building, they examined separately. Accordingly, displacements and forces on the minaret were more accurately determined. By performing seismic analysis, the necessary restoration and retrofitting proposals were evaluated to ensure

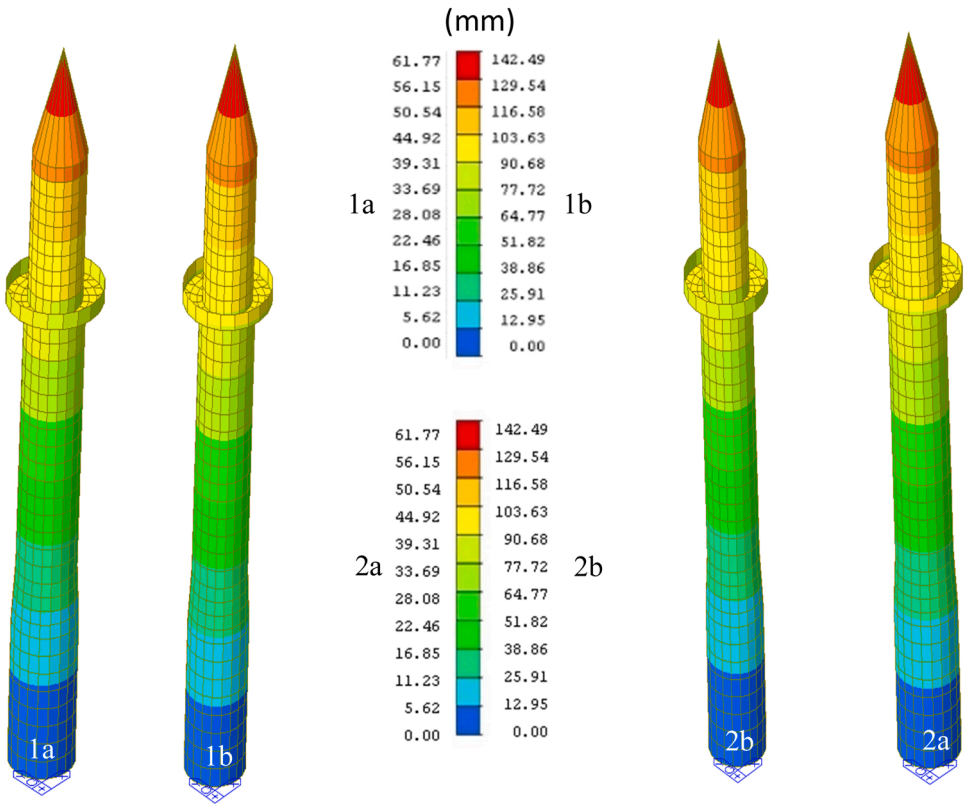


**Fig. 22.** Displacements observed in the minaret (1a:DD3 Exp, 1b: DD2 Exp, 2a:DD3 Eyp, 2b:DD2 Eyp).

**Table 16**
Displacement checking for control points of the minaret.

| Earthquake Level | Base shear (kN) | | Performance point (mm) | | Drift ratio | | Limit ratio | Check |
|---|---|---|---|---|---|---|---|---|
| | x | y | xp | yp | % | % | % | √ / × |
| DD3 | 37.2 | 37.2 | 51.0 | 51.0 | 0.295 | 0.295 | 0.3 (LD) | √ |
| DD2 | 38.1 | 38.1 | 120.0 | 120.0 | 0.695 | 0.695 | 0.7 (CD) | √ |

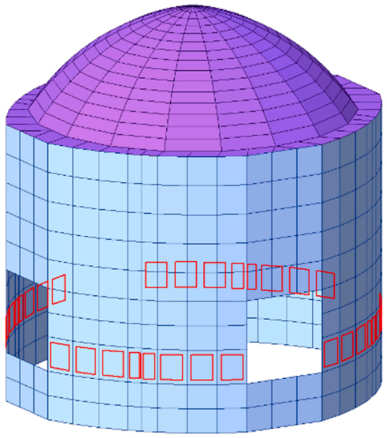

**Fig. 23.** Critical section on the masonry walls of the tomb (red-colored parts).

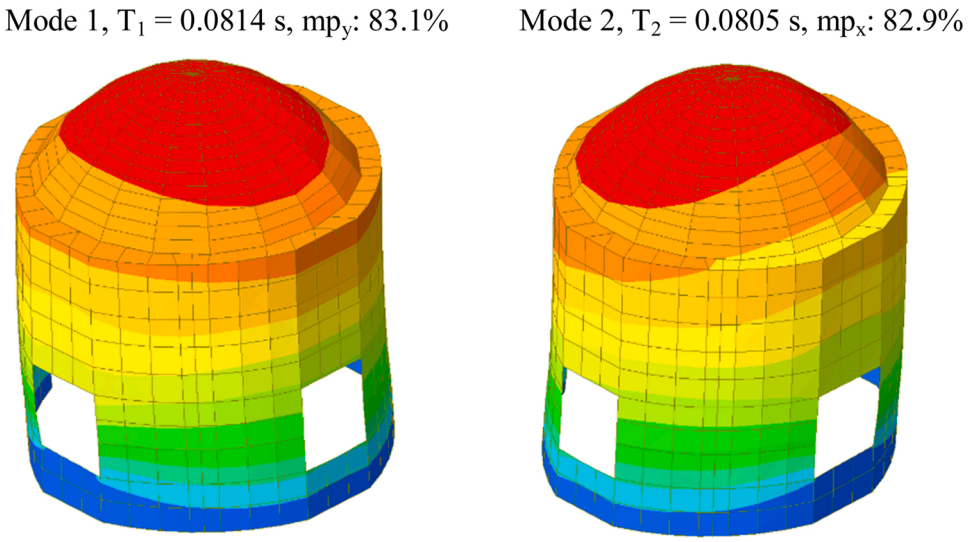


**Fig. 24.** Mod shapes ($mp_x$ and $mp_y$: mass participations in the x and y directions).

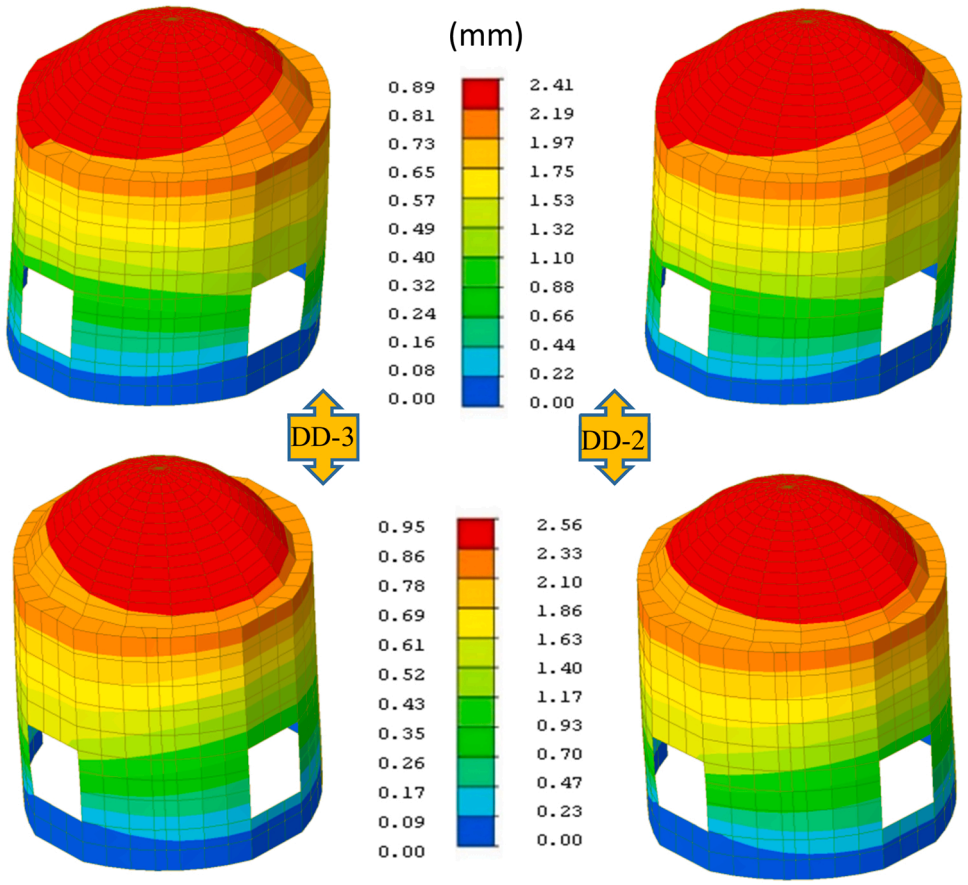


**Fig. 25.** Lateral displacements observed in the tomb structure.

**Table 17**
Inter-story drifts.

| Earthquake class | Displacement ΔD, (mm) | | Drift ratio, ΔD/H | | Limit | Check |
|---|---|---|---|---|---|---|
| | x | y | % | % | % | √ / × |
| DD3 | 0.8 | 0.8 | 0.020 | 0.021 | 0.3 (LD) | √ |
| DD2 | 0.1 | 2.3 | 0.003 | 0.057 | 0.7 (CD) | √ |

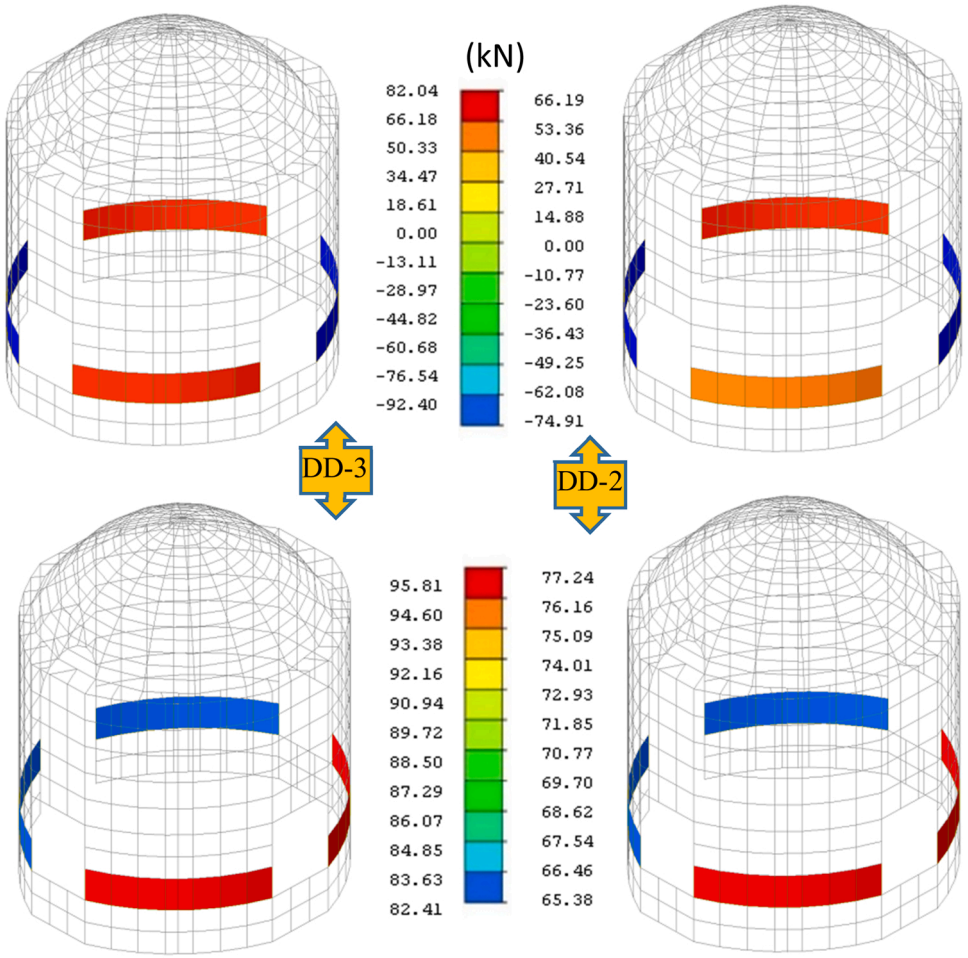


**Fig. 26.** Shear forces on the tomb under seismic effects.

**Table 18**
Seismic performance analysis results.

| Earthquake class | Ra | Shear force check | * % r | Target performance | Check |
|---|---|---|---|---|---|
| DD3 | 1 * * | √ | 0 | LD | √ |
| DD2 | 3 * * | √ | 0 | CD | √ |

* The ratios of the shear forces on the masonry walls failed in shear to the total shear force acting on the same story. * * According to the SRMGHS 2017.

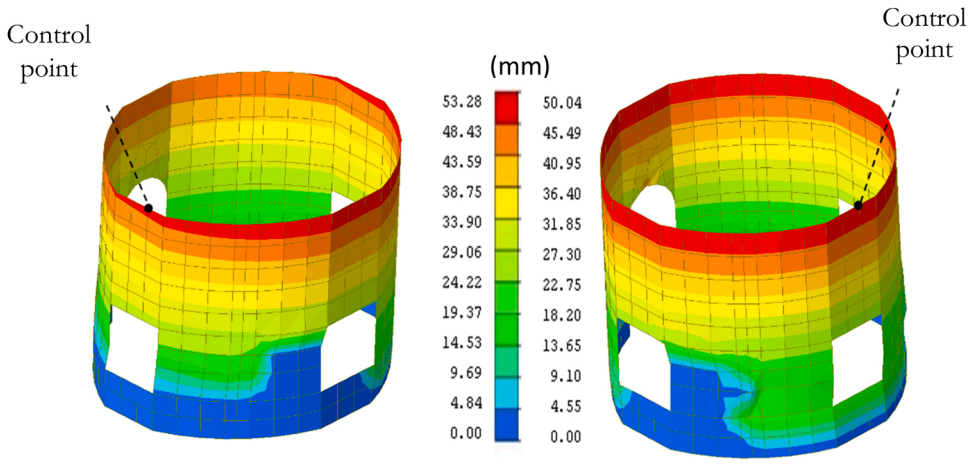


**Fig. 27.** Control points of the tomb for earthquake loads in the positive x (left) and y directions (right).

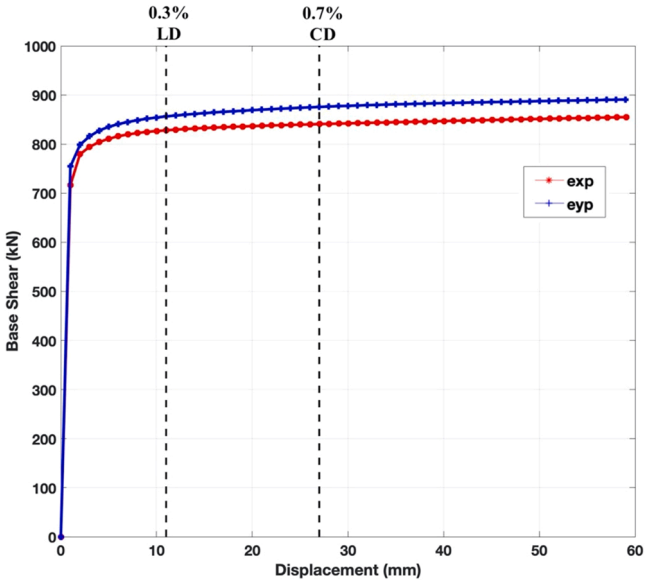


**Fig. 28.** Base shear vs. displacement.

this historically and culturally important mosque complex exists in the future. Our cultural values are, therefore, preserved.

## 5. Conclusions

Heritage masonry buildings convey historical construction knowledge to the present. However, to preserve the integrity of such buildings, restoration and conservation practices are needed. The first stage in a restoration practice is the review of any historic data and on-site examination of the building. Based on these examinations, the building surveys of the examined structures were prepared and facades and cross-sectional views were drawn. Numerical models of the structures were created using the finite element software according to these drawings and dead and live loads were defined. Mode shapes of the structures were determined by the modal analysis. Furthermore, inter-story drifts and performance assessment were done with the response spectrum analysis. The inter-story drift and shear force values were compared with the allowed values envisaged in the seismic code and the guide for historic structures for each ground motion level. The nonlinear analysis was performed under static loads applied in both directions and the obtained inter-story drift values were confirmed by comparing with the linear analysis results. Moreover, the local failure mechanisms on the facade walls of the main building, namely, overturning, lateral bending, and vertical bending mechanisms were examined.

This paper presents all stages of a post-restoration seismic performance assessment of a hypostyle mosque constructed in 1273. For this purpose, structural analyses were conducted following the restoration practice to assess the seismic performance. The seismic performance and global/local failure mechanisms were examined by linear, static pushover, and kinematic limit analyses.

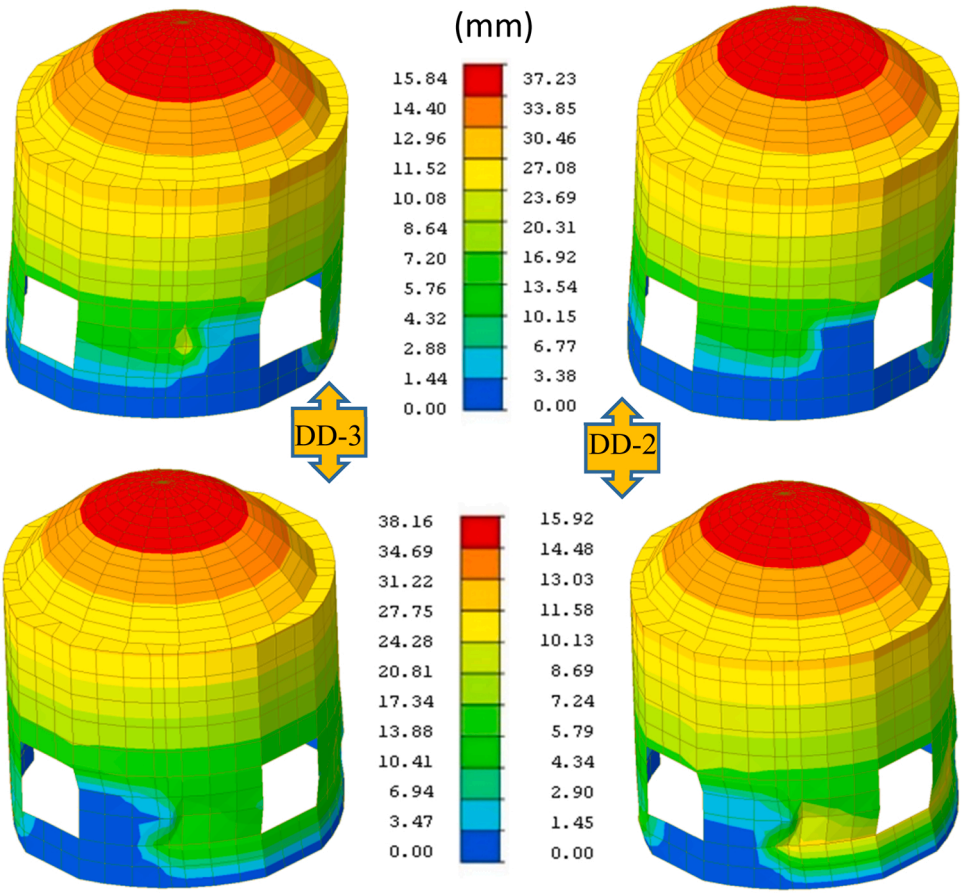


**Fig. 29.** Lateral displacements observed in the tomb structure.

**Table 19**
Displacement checks for control points of the tomb.

| Earthquake Class | Base shear (kN) | | Performance point (mm) | | Drift ratio | | Limit ratio | Check |
|---|---|---|---|---|---|---|---|---|
| | x | y | xp | yp | % | % | % | √ / × |
| DD3 | 828.1 | 856.3 | 11.0 | 11.0 | 0.275 | 0.275 | 0.3 (LD) | √ |
| 1 | 840.7 | 875.6 | 27.0 | 27.0 | 0.676 | 0.675 | 0.7 (CD) | × |

Accordingly, the main mosque building, the minaret, and the tomb were modeled separately and were analyzed under earthquake loads.

According to the structural analyses, the following key findings were obtained for three structures in the mosque complex:

- The linear performance analysis results revealed that the structure satisfies the limits values of inter-story drifts and shear forces for "Limited Damage" and "Controlled Damage" performance levels corresponding to DD-3 and DD-2 earthquakes, respectively.
- The displacement-controlled nonlinear analysis results indicated that the structure satisfies inter-story drift limits for "Limited Damage" and "Controlled Damage" performance levels corresponding to DD-3 and DD-2 earthquakes, respectively.
- Local collapse mechanisms on the main structure were obtained by the kinematic limit analysis. The results showed that overturning, lateral bending, and vertical bending mechanisms occur under DD-3 and DD-2 ground motions. However, since the facade walls were joined by clamps, it was decided that these mechanisms would not pose a risk.

Evaluations of the linear and nonlinear analysis results are shown in Table 20.

In conclusion, the authors suggest that the numerical analyses presented in this paper for this 750-year-old historic religious

**Table 20**
Summary of the analysis results for the main structure, the minaret and the tomb.

| **Main structure** | | | | | | | | | | |
|---|---|---|---|---|---|---|---|---|---|---|
| | **Compressive Stress** | | | **Tensile Stress** | | | **Shear Stress** | | **Story Drift Ratio** | |
| **L** | Vertical | Seismic | | Vertical | Seismic | | DD3 | DD2 | DD3 | DD2 |
| | | DD3 | DD2 | | DD3 | DD2 | | | | |
| | √ | √ | √ | √ | √ | √ | √ | √ | √ | √ |
| **P** | √ | √ | √ | √ | √ | √ | √ | √ | √ | √ |
| **Minaret** | | | | | | | | | | |
| | **Compressive Stress** | | | **Tensile Stress** | | | **Shear Stress** | | **Story Drift Ratio** | |
| **L** | Vertical | Seismic | | Vertical | Seismic | | DD3 | DD2 | DD3 | DD2 |
| | | DD3 | DD2 | | DD3 | DD2 | | | | |
| | √ | √ | √ | √ | √ | √ | √ | √ | √ | √ |
| **P** | √ | √ | √ | √ | √ | √ | √ | √ | √ | √ |
| **Tomb** | | | | | | | | | | |
| | **Compressive Stress** | | | **Tensile Stress** | | | **Shear Stress** | | **Story Drift Ratio** | |
| **L** | Vertical | Seismic | | Vertical | Seismic | | DD3 | DD2 | DD3 | DD2 |
| | | DD3 | DD2 | | DD3 | DD2 | | | | |
| | √ | √ | √ | √ | √ | √ | √ | √ | √ | √ |
| **P** | √ | √ | √ | √ | √ | √ | √ | √ | √ | √ |

L and P refer to Linear and Pushover analyses, respectively

structure built using a long-forgotten construction technique should be considered an effective and necessary step in the restoration of such historic buildings. Underestimating the numerical analysis stage might cause serious problems in terms of the sustainability of such structures.

## Declaration of Competing Interest

The authors declare that they have no known competing financial interests or personal relationships that could have appeared to influence the work reported in this paper.

## Data availability

No data was used for the research described in the article.

## Acknowledgements

The authors would like to thank Directorate General of Foundations, Kastamonu Regional Directorate and Mr. Burhan Kurtoğlu for their valuable supports. This study was performed by the courtesy of Republic of Turkey, Ministry of Cultural and Tourism, Directorate General of Foundations (Decision no. 230031 dated 11.04.2021)

## References

[1] M. Saba, E.E. Quiñones-Bolaños, A.L.B. López, A review of the mathematical models used for simulation of calcareous stone deterioration in historical buildings, Atmos. Environ. 180 (2018) 156–166.
[2] M. Saba, E.E. Quiñones-Bolaños, H.F.M. Batista, Impact of environmental factors on the deterioration of the Wall of Cartagena de Indias, J. Cult. Herit. 39 (2019) 305–313.
[3] M. Saba, L.N. Hernandez-Romero, J. Lizarazo-Marriaga, E.E. Quiñones-Bolaños, Petrographic of limestone cultural heritage as the basis of a methodology to rock replacement and masonry assessment: cartagena de Indias case of study, Case Stud. Constr. Mater. 11 (2019), e00281.
[4] M.C. Porcu, E. Montis, M. Saba, Role of model identification and analysis method in the seismic assessment of historical masonry towers, J. Build. Eng. 43 (2021), 103114.
[5] R.M. Alkadi, The origin of the islamic ribbed vaults famed in North Africa and Spain. PhD Dissertation, E. T. S. Arquit. (UPM) (2017).
[6] Y. Yaralov, Architectural monuments in Central Asia between 8th and 12th centuries, First Int. Congr. Tursiksh Arts, Ank., Turk. (1962).
[7] M. Taghavi, A.H. Gholam, Evaluation of Seljuk and Safavid d and Arrays Monuments in Qazvin, Adv. Environ. Biol. 9 (4) (2015) 204–220.
[8] Bakırer Ö. (1981) Brick usage in Anatolian architecture belonging to Seljuk era, Vol. 1, Ankara, ODTÜ Press.
[9] Unesco (1999) Report on State Historical and Cultural Park "Ancient Merv", No. 886.
[10] B. Ja. Staviskij, Arts of Central Asia, Iskusstvo, Moscow, 1974 (in Russian).
[11] G. Öney, Turkish period buildings in Ankara, Turkey (1971) 98–101.
[12] Y. Önge, Wooden Ceilings in Seljuks and Beylikler era, Turkish Historical Society, 1975 (in Turkish).
[13] R. Arık, Examples of Turkish Architecture in Westernization Period, Three Wooden Mosques Anatolia, Ank. (1973).
[14] O. Aslanapa, First Turkish Architecture in Anatolia, Beginning and Development, Ankara, Turkey, 2007 (in Turkish).
[15] G. Öney, Ankara Arslanhane Mosque, 10, 11, Ankara, Turkey, 1998 (in Turkish).
[16] K. Hayes, The Wooden Hypostyle Mosques of Anatolia: Mosque and State-Building under Mongol Suzerainty, PhD dissertation, METU, etd.lib, 2010, metu.edu.tr/upload/12612251/index.pdf.

[17] A. Erarslan, A wooden-columned mosque from Anatolia, Beyşehir Eşrefoğlu mosque, Bulletin of the Transilvania University of Braşov Series II, For., Wood Ind., Agric. Food Eng. 14 (2021) 63, https://doi.org/10.31926/but.fwiafe.2021.14.63.1.8.
[18] B. Yildizlar, B. Sayin, C. Akcay, A case study on the restoration of a historical masonry building based on field studies and laboratory analyses, 2020, Int. J. Archit. Herit. 14 (9) (2020) 1341–1359.
[19] T.S. Bozkurt, B. Sayin, C. Akcay, B. Yildizlar, N. Karacay, Restoration of the historical masonry structures based on laboratory experiments, J. Build. Eng. 7 (2016) 343–360, https://doi.org/10.1016/j.jobe.2016.07.010.
[20] R. Caponette, S. Sebastiano d'urso, R. Rosso, M. Seminara, Poggioreale: Urban monument to negligence restoration strategies, in: Proceedings of the 4th Biennial of Architectural and Urban Restoration, BRAU 4 Host of the Itinerant Congress Hidden Cultural Heritage: under Water, under Ground and within Buildings, 15–30 April 2018, 2018.
[21] ICOMOS (2001) Recommendations for the Analysis, Conservation and Structural restoration of architectural heritage, International scientific committee for analysis and restoration of structures of architectural heritage www.esicomos.org/Nueva./ISCARSAHSept2001.doc, Paris, France.
[22] The Burra Charter, The Australia ICOMOS charter for the conservation of places of cultural Significance, 2004.
[23] Declaration of Dresden, Reconstruction of Monuments Destroyed by War, ICOMOS, 1982.
[24] The Venice Charter, The Venice ICOMOS Charter for the restoration of historic monuments, in: Adopted at the Second International Congress of Architects and Technicians of Historic Monuments, Venice, Italy, 1964. ICOMOS.org/ch arters/venice_e.PDF.
[25] The Burra Charter Charter, The Australia ICOMOS Charter for Places of Cultural Significance 1999, Australia, 1999. icomos.org/publications/charters.
[26] M. Shariq, S. Haseeb, M. Arif, Analysis of existing masonry heritage building subjected to earthquake loading, Procedia Eng. 173 (2017) 1833–1840.
[27] B. Sayin, B. Yildizlar, C. Akcay, B. Gunes, The retrofitting of historical masonry buildings with insufficient seismic resistance using conventional and non-conventional techniques, Eng. Fail. Anal. 97 (2019) 454–463.
[28] S. De Silva, G.H.M.J.S. De Silva, H.M.S.S. Padmal, Assessment method for seismic vulnerability of old masonry buildings in Sri Lanka, Procedia Eng. 212 (2018) 61–68.
[29] B. Gunes, T. Cosgun, B. Sayin, O. Ceylan, Structural rehabilitation of a middle byzantine ruin and the masonry building constructed above the ruin. Part II: the building, Eng. Fail. Anal. 105 (2019) 527–544.
[30] A.E. Akan, G.Ç. Başok, A.E. Hilal, T. Örmecioğlu, S.Z. Koçak, T. Cosgun, O. Uzdil, B. Sayin, Seismic evaluation of a renovated wooden hypostyle structure: a case study on a mosque designed with the combination of Asian and Byzantine styles in the Seljuk era (14th century AD), J. Build. Eng. 43 (2021), 103112.
[31] B. Yildizlar, Seismic performance analysis and rehabilitation applications for a historical masonry building through field works and experimental investigations, Structures 34 (2021) 1811–1833.
[32] M. Betti, L. Galano, Seismic analysis of historic masonry buildings: the vicarious palace in Pescia (Italy), Buildings 2 (2) (2012) 63–82.
[33] G. Milani, G. Venturini, Automatic fragility curve evaluation of masonry churches accounting for partial collapses by means of 3D FE homogenized limit analysis, Comput. Struct. 89 (17–18) (2011) 1628–1648.
[34] C. Akcay, T.S. Bozkurt, B. Sayin, B. Yildizlar, Seismic retrofitting of the historical masonry structures using numerical approach, Constr. Build. Mater. 113 (2016) 752–763.
[35] G.Ö. Özen, Comparison of elastic and inelastic behavior of historic masonry structures at the low load levels, Master of Science Thesis, Middle East Tecnical University, Inst. Sci. Technol. (2006).
[36] M. Betti, A. Vignoli, Assessment of seismic resistance of a basilica-type church under earthquake loading: Modelling and analysis', Adv. Eng. Softw. 39 (4) (2008) 258–283.
[37] G. Milani, P.B. Lourenco, A. Tralli, 3D homogenized limit analysis of masonry buildings under horizontal loads, Eng. Struct. 29 (2007) 3134–3148.
[38] N.C. Palazzi, L. Rovero, U. Tonietti, J.C. De la LIera, Kinematic limit analysis of basilica del Salvador, a significant example of neo-gothic architecture in Santiago, Chile, 16th Eur. Conf. Earthq. Eng., Thessalon., Greece (2018) 2018.
[39] P.G. Asteris, M.P. Chronopoulos, C.Z. Chrysostomou, H. Varum, V. Plevris, N. Kyriakides, V. Silva, Seismic vulnerability assessment of historical masonry structural systems, Eng. Struct. 62 (2014) 118–134.
[40] A. Karic, J. Atalić, A. Kolbitsch, Seismic vulnerability of historic brick masonry buildings in Vienna, Bull. Earthq. Eng. (2022) 1–29.
[41] C. Maraveas, Assessment and restoration of an earthquake-damaged historical masonry building, Front. Built Environ. 5 (2019) 112.
[42] R.S. Olivito, S. Porzio, A new multi-control-point pushover methodology for the seismic assessment of historic masonry buildings, J. Build. Eng. 26 (2019), 100926.
[43] M.L. Kındığılı, An example of wooden post mosque from Erzurum-Askala Güllüdere (Pırtın) Village, J. Turk. Res. Inst. TAED 64 (2019), https://doi.org/10.14222/Turkiyat4002.
[44] E. Atak, An example of wooden columned structure in Tokat: the great mosque of Üzümören, J. Vakıflar 51 (2019) 99–130.
[45] F. Karakuş, Evaluation study on wooden pillar mosques built in Anatolia in the 13th century, The Turkish Online Journal of Design, Art. Commun. 11 (1) (2021) 131–161.
[46] M.A. Faruq, Seljuqi mosque planning styles and their effect on the planning of Iraqi mosques, Al-Adab, Journal 103 (2013) 289–314.
[47] F.A. Mustafa, A.S. Hassan, Mosque layout design: an analytical study of mosque layouts in the early Ottoman period, Frontiers of Architectural, Research 2 (4) (2013) 445–456.
[48] O. Aslanapa, Seljuk Masjids and Wooden Mosques in Anatolia. Turkish Art and Architecture, Praeger Publisher, New York, 1971, pp. 119–123.
[49] I. Unutmaz, Eşrefoğlu Süleyman Bey Mosque with wooden pillar in Beysehir, Hist. Soc. 8 (47) (1987) 31–35.
[50] Karamağaralı, B. (1993). Ayaş Ulu Mosque. Ayaş ve Bünyamin Ayaşi, Symposium on Ayaş ve Bünyamin Ayaş-i in history and today, 2–4 July 1993). Ankara. 53–59 (in Turkish).
[51] M.K. Şahin, Şeyh Habil Village Mosque in Çarşamba/Yaycılar district of Samsun. Atatürk University, J. Soc. Sci. Inst. 4 (2) (2004) 15–36.
[52] M. Ahmad, K. Rashid, N. Naz, Study of the ornamentation of Bhong Mosque for the survival of decorative patterns in Islamic architecture, Front. Arch. Res. 7 (2) (2018) 122–134.
[53] R. Othman, Z.J. Zainal-Abidin, The importance of islamic art in mosque interior, Procedia Eng. 20 (2011) 105–109.
[54] M. Rustamova, Wood and stone columns of ruined and destroyed mosques of Central, Asia 3 (9) (2019) 31–61, https://doi.org/10.33404/anasay.573833.
[55] Midas Gen, in: Integrated Solution System for Building and General Structures, MIDAS Information Technology Co, 2018.
[56] PRO_CINEm, Analysis of Local Mechanisms through Linear and Nonlinear Kinematic Analysis Software, 2Si Software e servizi Per L'ingegneria, Italy, 2019.
[57] B.Ya Staviskij, Arts of Central Asia, Iskusstvo, Moscow, 1974 (in Russian).
[58] V. Nusov, Architecture of Kyrgyzia from Ancient Times till Today, Frunze, Kyrgyzstan, 1971.
[59] G. Öney, Ankara'da Selçuklu ve Beylikler Devri Ahsap Malzemeli Cami ve Mescitler, Yapı Kredi Press, Istanbul, Turkey, 1994, pp. 73–86.
[60] G.A. Pugaçenkova, South Turkmenistan Archeology in Relation to Slavery and Feudalism Era, Akademiya Nauk Publications, Moscow, 1958.
[61] A. Gökoğlu, Paphlagonia, Kast. Prov. (1952) 193–267.
[62] Çiftçi F., Mosques, tombs and other historical assets of Kastamonu province, Municipality publishing, 91–93 (in Turkish).
[63] K.K. Eyüpgiller, The history of a city: Kastamonu, Eren publishing, Istanbul (1999) 58–63.
[64] Y. Yücel, Çobanoğulları Beylikleri, Ankara (1980).
[65] T.M. Yaman, History of Kastamonu: until the end of 15th century, Ahmed İhsan Press (1935).
[66] T.R. DGF, Restoration Report of Atabey Gazi Mosque, T. R. Dir. Gen. Found. Arch. (2020).
[67] TBEC (2018) Turkey Building Seismic Code: Rules for design of buildings under earthquake effect, Official Gazzette, 18.03.2018, 30364 (in Turkish).
[68] SRMGHS (2017) Seismic Risks Management Guide for Historic Structures, General Directorate of Foundations, Ankara, Turkey (in Turkish).
[69] ICOMOS-ISCS: Illustrated glossary on stone deterioration patterns, 2008. Accessed on openarchive.icomos.org/id/eprint/434/1/Monuments_and_Sites_15_ISCS_Glossary_Stone.pdf.

[70] Web site (2022) The yearbooks of Kastamonu province dating with 1286, 1310, 1311, 1312, 1314 and 1317 (muslim calender), Available at: kastamonur.com/1314-senes-kastamonu-vlayet-salnames8/.
[71] M. Behçet, Ancient assets of Kastamonu province (Kastamonu Asar-ı Kadimesi), Istanbul, Matbaa-i Amire 1341 (1998) 51–55.
[72] AFAD (2020) Turkey Earthquake Risk Map Interactive Web Application. Available at: tdth.afad.gov.tr/TDTH/main.xhtml.
[73] D.F. D'Ayala, E. Speranza, Definition of collapse mechanisms and seismic vulnerability of historic masonry buildings, Earthq. Spectra 19 (2003) 479–509.